Fabrication and Investigation of Nickel-rich (Lithium Nickel Manganese Cobalt Oxide) Electrode Materials

By

Muhammad Kamran Khan

Supervised by

Dr. Muhammad Arshad

Principal Scientific Officer

Nanosciences and Technology Department,

National Centre for Physics (NCP), Islamabad.

2021-23

This work is submitted as a dissertation in partial fulfillment of the requirement for the degree of

MASTER OF PHILOSOPHY

IN

PHYSICS

To The

Department of Physics

Quaid-i-Azam University Islamabad, Pakistan

2021-23

Research Completion Certificate

It is certified that research work contained in the thesis titled **"Fabrication and Investigation of Nickel-rich (Lithium Nickel Manganese Cobalt Oxide) Electrode Materials"** has been carried out and completed by **Mr. Muhammad Kamran Khan** Reg No: **02182113030** under my supervision at Nanoscience and Technology Department National Centre for Physics (NCP), Quaid-i-Azam University Islamabad (Pakistan).

Supervisor: _____

Dr. Muhammad Arshad

Principal Scientific Officer

Nanosciences and Technology Department,

National Centre for Physics (NCP), Islamabad.

Chairman: _____

Prof. Dr. Kashif Sabeeh

Chairman Department of Physics,

Quaid-i-Azam University, Islamabad.

Declaration

I hereby declare that the thesis titled “Fabrication and Investigation of Nickel-rich (Lithium Nickel Manganese Cobalt Oxide) Electrode Materials” submitted to the Department of Physics, Faculty of Natural Sciences, Quaid-i-Azam University for the award of Degree of Master in Philosophy is the result of research work carried out by me under the supervision of principal scientific officer **Dr. Muhammad Arshad** during the period 2022-23. I further declare the results in this thesis are original and that no part of this thesis falls under plagiarism. I shall be responsible for any copyright violation found in this work.

Muhammad Kamran Khan

Registration No: 02182113030

Signature: _____

DEDICATION

This dissertation is dedicated

to

My Loving Parents, Teachers, my Siblings

and research colleagues who helped me a lot to get this work

I am thankful for their everlasting support and encouragement.

ACKNOWLEDGMENT

In the name of Allah Almighty, the most merciful and beneficent, who owns all the knowledge. It is a matter of utmost pleasure for me to complete my thesis after a long-term effort and mind work**.** I want to express my gratitude to my respected supervisor **Dr. Muhammad Arshad** Nanosciences and Technology Department National Centre for Physics (NCP) Islamabad, for his encouragement, guidance, and support throughout my thesis work. It has been an honor and pleasure to work with such a great supervisor. This research work would not be possible without his kind help. I am thankful to the chairman, Department of Physics **Prof Dr. Kashif Sabeeh**, who supported me in completing my research under my respected supervisor **Dr. Muhammad Arshad.**

I would like to give special thanks to my respected parents who have ever-present love, kindness, prayer, support, upbringing, faith and encouragement has made me the person I am today. I am very thankful to my respected parents who has supported and encouraged me throughout my study career. Indeed, it was the prayers of my beloved mother and dear father. After my parents, I am grateful to my brothers and sisters whose love and care for me to support complete this project. I am also thankful to my brother Irfan Khan, who gave me valuable ideas and encouragement to complete this work. I wish to express my sincere thanks to my colleagues for their support and encouragement. Their guidance and support were important throughout my research work. Lastly, I offer my regards and blessing to all of those who supported me in any aspect during the completion of this research work.

Muhammad Kamran Khan

Fabrication and Investigation of Nickel-rich (Lithium Nickel Manganese Cobalt Oxide) Electrode Materials

Contents

List of Figures

List of Tables

Abstract

Scientists and researchers are concentrating on cathode materials with enhanced nickel content in layered oxides for lithium-ion batteries due to their increased energy density and capacity. Consequently, this study successfully generated the cathode material $LiNi_{0.8}Mn_{0.1}Co_{0.1}O_2$ (NMC811). However, these nickel-rich cathode materials continue to face commercialization challenges including structural instability, structural deterioration, microcracks, increased reactivity with electrolytes, as well as worries about electrochemical and thermal stability. We have successfully produced lithium nickel manganese cobalt dioxide (NMC811) in our continuing study using a two-step process that includes co-precipitation and solid-state synthesis methods. Subsequent to fabricating the NMC811 cathode, we employed the molten salt etching technique to generate MXene ($Ti_3C_2T_x$), which was applied as a coating on NMC811 to enhance its conductivity. (Its reduced reactivity on the lower surface enhances cycling durability, mitigates crack formation following repeated cycles, and promotes the growth of lithium dendrites). Properties of MXene coated (NMC811) characterized by XRD, SEM, EDX, CV and EIS. The structure, geometry of samples and crystallinity were confirmed by X-ray diffraction. The morphology, shape and size of nanoparticles are revealed by scanning electron microscopy. Analysis of the elemental composition of nanoparticles were investigated by EDX. The CV curve exhibit redox behaviour of cathode material (NMC811) and composite of CV curves has shown that conductivity has been increased due to the coating of MXene. EIS plots indicate that due to coating of MXene on active electrode material (NMC811), decrease its impedance between electrode/electrolyte interface layer, and enhance Li^+ ion transportation between electrodes.

Chapter No. 1

Introduction

In this chapter we have discussed energy issues and how new energy storage devices globally can reduce those issues. Brief introduction of energy storage devices and explanation of advanced rechargeable lithium-ion batteries and their cathode materials. Later on, we have discussed the challenges that facing by a lithium-ion batteries, and how these challenges solve by nickel-rich cathode materials. At the end, we have briefly explained $LiNi_{0.8}Mn_{0.1}Co_{0.1}O_2$ (NMC811) cathode material, its properties problems and solution of those problems. Finally, in this chapter we have given a brief review of MXene ($Ti_3C_2T_x$) and nano-composite of NMC811 with $Ti_3C_2T_x$ (NMC811- $Ti_3C_2T_x$).

1.1 Introduction

LIBs are formed from one or more generating components known as cells. Positive electrodes, negative electrodes, and an electrolyte (that located among two electrodes) are the three Sun is a natural source of renewable energy because H_2 and He_2 gases are burned in space. Whereas non-renewable energy source, as an example of a fossil fuel is coal, natural gas, and oil. Coal and gas release SO_2 when burned, which polluted the environment. Fossil fuels are also the cause of climate change and long-term temperature change which disturb the weather pattern that' results actually global warming. A factor that is part of climate change is global warming, which is the gradual increase in the planet's temperature. It is imposed on by a rise in greenhouse gas concentrations in the atmosphere, mainly as a result of human activities like farming and the burning of fossil fuels. The development of electric vehicles (EVs) has been facilitated by both global warming and the depletion of fossil resources. Furthermore, power electronics industries' rapid growth has resulted in the realization of high energy-efficient vehicles. Because public transport consumes a lot of energy, EVs are good source to lower greenhouse gas emissions [1].

The number of flexible energy-storage devices is growing in popularity because of their distinct, and lightweight devices. Soft products, roll-up displays, and wearable devices are examples of wearable electronic devices. In recent years, maximum work has been put into fulfilling the standards of significant progress has been made towards flexible energy storage systems. However, current energy-storage modules made of supercapacitors and lithium-ion

batteries are often too heavy, inflexible, and bulky to meet the specific needs of flexible electronics. As a result, the next wave of energy storage device development will focus on producing thin, little units that are adaptable, having stylistic variety, and good mechanical characteristics. Lithium-ion batteries and flexible supercapacitors are two specimen of flexible energy storage systems., must be fulfilled and improved [2].

Lithium-ion batteries are outstanding source of energy in portable electronics, are expanding rapidly into the grid-energy storage sector as well as the market for electric vehicles. Balancing various performance aspects such as energy efficiency, power output, longevity, affordability, safety, and ecological impact necessary, depending on the specific application. The technology today for lithium-ion batteries is based on organic liquid electrolytes and electrodes for insertion reactions. Development of solid electrolytes, lithium metal anodes, and novel electrode materials that combine insertion and conversion processes [3].

Components that make up each cell. Lithium cobalt oxide ($LiCoO_2$) or lithium iron phosphate ($LiFePO_4$) constitutes the positive electrode, while the negative electrode is crafted from carbon (graphite). The selection of the electrolyte differs depending on the particular battery type [4]. Positive electrode, known as the cathode, and the negative electrode, known as the anode, within a standard Li+-ion cell, are both in contact with an electrolyte containing lithium ions. Electrodes are kept away from one another by a separator, often a microporous polymer membrane, this supports lithium ion exchange but not electron exchange between the two electrodes [5].

LIBs are one of the most top ranked energy storage technologies since 2015. More efficient, high specific capacity, energy and power density and good cycle life are properties of lithium-ion batteries. LIBs widely used in electronics product such as EVs, HEVs, electronics watches, mobile phones, notepad, laptops, e-bike [6].

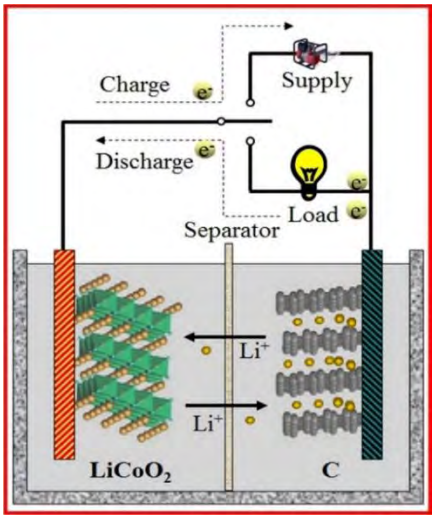

Figure 1.1 Lithium-ion battery fundamental parts and functionality [5]

High capacity and high energy density materials are still mandatory to increase lithium-ion battery performance. Transition metal oxide such as $LiCoO_2$, $LiMnO_2$, three transition metals (NMC) as cathode materials for lithium-ion batteries, and $LiMnPO_4$ and $LiCoPO_4$ are two more phosphates utilized as commercial cathodes in lithium-ion batteries. Nickel-rich layered (TM) oxide electrode materials ($LiNi_xCo_yMn_zO_2$) ($N_xM_yC_z$ $x + y + z = 1$, $x > 0.5$)) have their high operating voltage and large capacity as benefits. Due to their higher capacity(200Ah/kg), nickel-rich (NMC) cathodes (Ni >80%) have recently obtained interest. Nickle rich layered transition metals oxide having 250mAh/g specific capacity with 4.5V (during Li^+ ion intercalation and de-intercalation). Discharge voltage is 3.8V, while (NMC811) have average high capacity is 200mAh/g with 2.8V to 4.5V (during Li^+ ion intercalation and de-intercalation). NMC811 is getting a lot of interest in lithium-ion batteries cathode materials because of its outstanding electrochemical performance. A lot of attention has been enhanced by $LiNi_{0.8}Co_{0.15}Al_{0.05}O_2$ to improve lithium-ion battery energy density [7].

However, the widespread commercialization of NxMyCz or NCA based lithium-ion batteries faces significant challenges due to rapid capacity degradation and a high risk of overheating. Incorporating higher levels of nickel (Ni) in NxMyCz or NCA can increase the specific capacity, but it also leads to issues with cycling stability and thermal stability, which is a major concern. The reaction of lithium compounds, such as LiPF6 and LiOH, generates hydrogen fluoride (HF), a key factor in TM-dissolution. Additionally, the mixing of Ni^{2+} cations cause Li/Ni site exchange and further capacity loss. Dissolved transition metal ions, along with oxidative byproducts of the electrolyte, can infiltrate the anode side due to chemical

interactions, resulting in degradation of the solid electrolyte interphase (SEI) layer on the graphite surface [8].

Researchers are currently working hard to increase the cycle stability of multilayer nickel-rich cathodes of synthesis conditions, ion doping, surface coating and electrolyte formulating. The most intriguing aspect is that lithium-ion battery electrochemical capabilities can be considerably improved by adding functional additives (substance that are added to protecting the formulation of the material from thermal and light-assisted oxidation at low concentrations) [7].

1.2 Energy storage devices

Energy storage devices play a crucial role in modern society by enabling the efficient utilization of energy resources and the integration of renewable energy sources into the power grid. These appliances support balance supply-demand dynamics and guarantee a steady and dependable energy supply. By enabling periodic energy sources, wind and solar might become widely used, covering deserts with solar panels and fields with wind turbines. Pumped hydroelectric storage (PHS), the most established and widely recognized energy storage method to date since its inception in 1929, boasts an installed capacity of 20.36 GW. CAES systems are high-efficiency combustion turbine facilities. It stays underground in a geologic formation until energy is required, at which point it is released, heated, passes through a turbine, and produces electricity. Although flywheels have been around for centuries, they have only recently come to be identified as types of bulk energy storage. Although they are expensive, these devices are very effective, quick to react, flexible to huge sizes, and environmentally friendly. Lead acid batteries are among the earliest and best-known types of electrical energy storage. Due in part to its inexpensive price and comparatively great efficiency, but restrained by its short cycle lifespan and poor performance at high temperatures [9].

Nickel-electrode batteries have minimal maintenance requirement and a high specific energy, but they are expensive and have a rather short cycle life. The world's largest battery installation was a Ni-Cd array capable of delivering 40 mega-watt of power for 7 minutes. However, in recent times, lithium-ion batteries have garnered significant popularity due to their exceptional efficiency, high energy density, power density, and cell voltage compared to other battery systems. But many large-scale systems haven't been created because of their huge capital costs. Lithium-ion designs are stronger and less chemically reactive than other lithium-based designs, which often use metallic lithium, which is extremely poisonous. Like the sodium sulphur battery, the sodium nickel chloride battery is a "molten salt" technology. It is more

resistant to overcharging and deep draining than its parent device, the NaS-battery, and may thus be a safer device. But it also has less strength and energy than NaS-devices, density. The Polysulfide-bromide batteries (PSB) device's power and energy capacity are virtually independent, as with previous flow battery technologies, making the system easily scalable and extremely flexible [8].

1.3 Batteries and their types

Figure 1.2 Primary batteries (Alkaline batteries, silver oxide batteries & secondary batteries (Lithium-ion battery) [10]

In 1800, A. Volta developed the first battery (voltaic pile). It was non-rechargeable battery. After that battery and its evolution begins and multiple batteries designed and that approach will enter into secondary battery (rechargeable battery). Battery should have high energy density, power density with high specific capacity for efficient output. We have state-of-the-art batteries engineered to meet the distinct demands of various devices, including energy grid stations for electric vehicles (EVs), hybrid electric vehicles (HEVs), and beyond etc. [10].

A power source that consists of one or more electrochemical cells coupled to an external source to power an electric device is known as an electric battery. An electrical object such as a penlight, a mobile phone, or an alternative fuel vehicle can be powered by a battery. An external electrical connection will allow ions from the positive electrode to flow to the negative terminal. Upon connecting the battery to an external electrical load, a redox reaction occurs. This transformation changes high-energy reactants into low-energy products, enabling the

discharge of the disparity in free energy as electrical energy into the external circuits. Electronic applications have long been connected to advancements in battery technology. Microelectronics and technological advancements like the transistor have pointed out the need for batteries with increased energy density, greater lifespans, and leak-free construction [11].

Following are component of a battery:

- Anode
- Cathode
- Electrolyte
- Container
- Collectors

Anode is the negative electrode. Cathode is the positive electrode. Electrolyte provides a medium through which positive ions can flow. Steel can that acts as the cathode's container and holds the components for the electrochemical process. Collectors act as connecting parts that gather the electrical current produced at the electrodes and link it to other circuits.

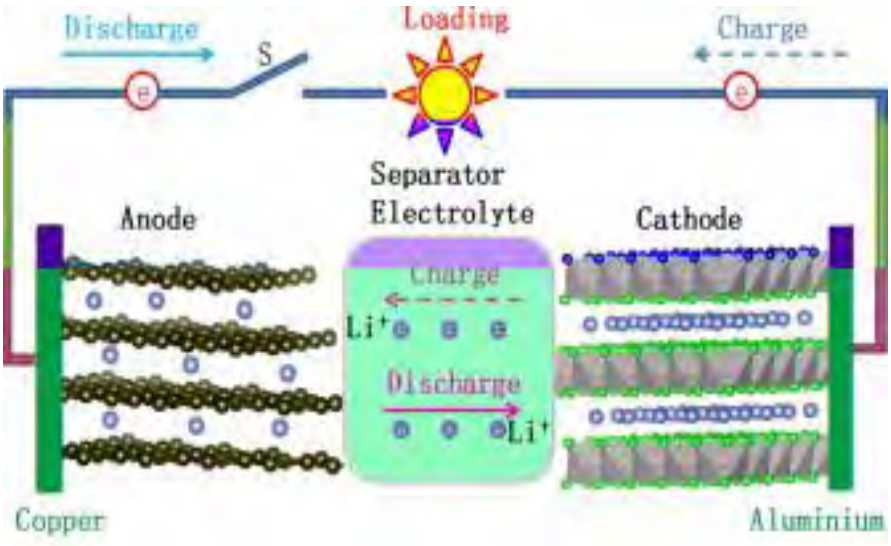

Figure 1.3 Components of battery [11]

Two types of batteries:

1.3.1. Primary Battery

Batteries which can-not be recharged called primary battery. The zinc carbon dry-cell serves as a widely used small-scale electrical energy source. Its electrolyte consists of a moist

paste containing zinc chloride and ammonium chloride, which functions as a salt bridge. It produces 1.5V. At anode oxidation occur zinc lose electrons:

$Zn \rightarrow Zn^{2+} + 2e$

At cathode manganese dioxide is reduced by gaining electrons:

$2MnO_2 + 2e \rightarrow Mn_2O_3 + H_2O$

Performance and lifespan are optimized in the alkaline cell. Compared to zinc carbon dry-cell, alkaline cell is designed for more high capacity. Its life is 5 times more than zinc carbon dry-cell. Button cells (primary battery) are useful in watches, some calculator and remote car etc. Silver zinc cells and lithium cells are example of button cells, produces 1.6V and 3V respectively. Alkaline batteries, silver oxide batteries, aluminum air batteries are primary batteries.

1.3.2. Secondary Battery

Battery which is used multiple time (rechargeable), called secondary batteries. Lead-acid batteries, alkali ions batteries, lithium-ion batteries. Electrical energy supplied by a charger (while charging) is converted into chemical energy (while discharging) in rechargeable cell (battery). Lead acid battery (car battery) is most widely used type of secondary cell. They are relatively cheap with good electrochemical properties. In this battery six distinct cells are serially arranged. Four negative electrodes are present, and three positive electrodes with sulfuric acid as electrolyte. Each cell consists of 2V, so total 12V (connecting 6 cells in a series) in this battery.

Anode:

$Pb + SO^{2-} \rightarrow PbSO_4 + 2e$

Cathode:

$PbO + SO_4 + 4H^{+} + 2e \rightarrow PbSO_4 + 2H_2O$

Nickel cadmium battery (NiCd) and Ni-MH (nickel metal hydrate) are also secondary batteries. But more efficient and most prominent is lithium-ion battery (LIB) that is used in widely due to its outstanding electrochemical performance [11].

1.4 Lithium-ion battery

First rechargeable lithium-ion battery developed by Whittingham in 1976. Its battery cathode was made up of TiS_2 and its anode was made up of lithium anode. At early stages that was not proper working due Li^+ dendrite formation on the anode surface and short circuiting after some time. Besenhard suggested cathode as a positive electrode and anode as a negative electrode for lithium-ion batteries. In the same year Goodenough introduced graphite as anode material and $LiCoO_2$ as a cathode material for lithium-ion battery. $LiCoO_2$ cathodes seems to be more durable than Na and other metals and outstanding electrochemical performance [12].

Goodenough was first to suggest stacked $LiCoO_2$ has high energy density, and voltage cathode material. In 1983, he also recognized manganese (Mn) spinel has cost effective cathode material. Besenhard, Yazami and Basu were discovered graphite, also with layered structure good anode material for Li^+ ion intercalation and de-intercalation in 1980s. Yoshino et al., in 1987, developed a with cell $LiCoO_2$ as the cathode and carbonaceous anode. Both the carbon anode and $LiCoO_2$ cathode are stable in air, proving to be promising materials for lithium-ion batteries. Lithium-ion battery has continuously improved, attracted a lot of scientific interest since 1990s and become an integral part of our daily lives [13].

A variety of secondary batteries (lithium-ion battery) with solid lithium anodes and a liquid organic electrolyte have been announced over the past few decades. Li-TiS_2, Li-$NbSe_3$, Li-MnO_2, Li-SO_2, and Li-MoS_2 are all on the list. Lithium-ion battery has a high energy density. With 3.6V operating voltage per cell, each cell may replace three NiCd or Ni-MH (metal hydride) batteries. Depending on cell size and structure, energy density has increased from 180 Wh/kg to as much as 330 Wh/kg. LIBs have important function in a variety of areas, including the development of electric cars, load balancing, and energy storage (solar, wind etc.) [12].

Important problems for modern lithium-ion battery are overcharge, which usually comes on by defective cell chargers. Overcharging a battery can cause thermal runaway, which can result in fire or explosion of the batteries. To achieve a high protection from overcharge the shuttle's oxidation potential should be slightly lower than the electrolyte's oxidation and decomposition potential and slightly greater than the cathode's end-of-charge potential. Thermal runaway is typically associated with temperature increases that are mostly caused by heat generation from the outside or the inside during extreme misuse. Positive temperature coefficient (PTC) devices are frequently included as parts of commercial batteries in order to prevent thermal runaway. The positive temperature coefficient devices can reversibly remain

conductive after cooling down. Most common causes of internal short circuits in lithium-ion batteries are the production of dendritic lithium. Battery short circuits will result from lithium dendrites growing on the anode's surface damaging the polymer separator and connecting the positive and negative electrode. Al, Cu, and Fe may be the main conductive metals responsible for internal short circuits in modern lithium-ion battery components. Therefore, the most crucial and efficient way to address the previously mentioned safety issues is to decrease the flammability of the organic liquid electrolyte by adding a flame-retardant electrolyte additive [14].

Particularly, Li $(Ni_xMn_yCo_z)O_2$ is known as NMC, new cathode material in research market. Thackeray et al., worked out to spinel structure of $LiMn_2O_4$, he reported $LiMn_2O_4$ is a more stable cathode material than $LiCoO_2$, Mn is less expensive than Co. Mn is dissolved in electrolyte at high temperature. Goodenough group creates thermochemical cathode notably known as $LiFePO_4$. Its redox potential 3.5V during Li^+ ions during intercalation and de-intercalation, but it has good thermal stability. $LiCoO_2$ has 4V (Li^+ /Li) but its bad thermal stability. Researches are struggling to sort out solution of $LiCoO_2$ thermal stability via doping with nickel, manganese and other transitions metals. Many researches created to improve the $LiNi_xMn_yCo_zO_2$ (NMC) cathode, due to its high energy density [15],[10].

1.5 Working Principle of Lithium-ion battery

Three basic parts make up a battery anode, cathode, and electrolyte. Common lithium-ion battery cathodes are typically lithium metal oxides like $LiCoO_2$, Li (NMC), nickel-rich in which nickel concentration more than 0.5 and graphite (carbonaceous) anode. While electrolytes are lithium salts like LiCl, Li_2CO_3, $LiPF_6$, LiOH etc. Commonly cathode materials, (LCO) and (LFP) used in lithium-ion batteries. Anode is consisting of graphite and electrolytes are different that depend on anode and cathode materials of lithium-ion battery [16].

During charging (electrical energy converted into chemical energy) process Li^+ ions travel towards anode from cathode via electrolyte through a separator, while electrons move from wire and reach at anode. In this way chemical energy stored in battery.

Cathode:

$$LiCoO_2 \rightarrow Li^+ + CoO_2 + e^- \quad \text{(oxidation)}$$

Anode:

$Li^+ + e^- + C_6 \rightarrow LiC_6$ (reduction)

Complete reaction:

$C_6 + LiCoO_2 \rightarrow LiC_6 + CoO_2$

During discharging (chemical energy converted into electrical energy) process Li^+ ions travel towards cathode from anode via electrolyte through a separator, while electrons move from wire and reach at cathode.

Cathode:

$Li^+ + CoO_2 + e^- \rightarrow LiCoO_2$ (reduction)

Anode:

$LiC_6 \rightarrow Li^+ + e^- + C_6$ (oxidation)

Complete Reaction:

$LiC_6 + CoO_2 \rightarrow LiCoO_2 + C_6$

Oxidation and reduction phenomena take place on both electrodes in alternatively. While undergoing the charging process, a voltage is applied across the electrodes. This voltage compels lithium ions to disperse into the electrolyte and insert themselves between the layers of graphene within the anode. Conversely, during the discharge process, lithium ions are integrated into the cathode's structure via the electrolyte. In addition, the electrolyte forces electrons to go through the wires in the outside circuits [12].

LIBs come with electronic collectors built-in. Rechargeable batteries are safe to use since they include protections against overcharging and overheating. The battery is completely charged and ready for use when the ion flow stops. During the charging and discharging operations, ions may migrate between the anodes and cathodes of rechargeable batteries, allowing energy to flow in and out. In lithium-ion batteries, the voltage reaches its maximum level when they are fully charged [13].

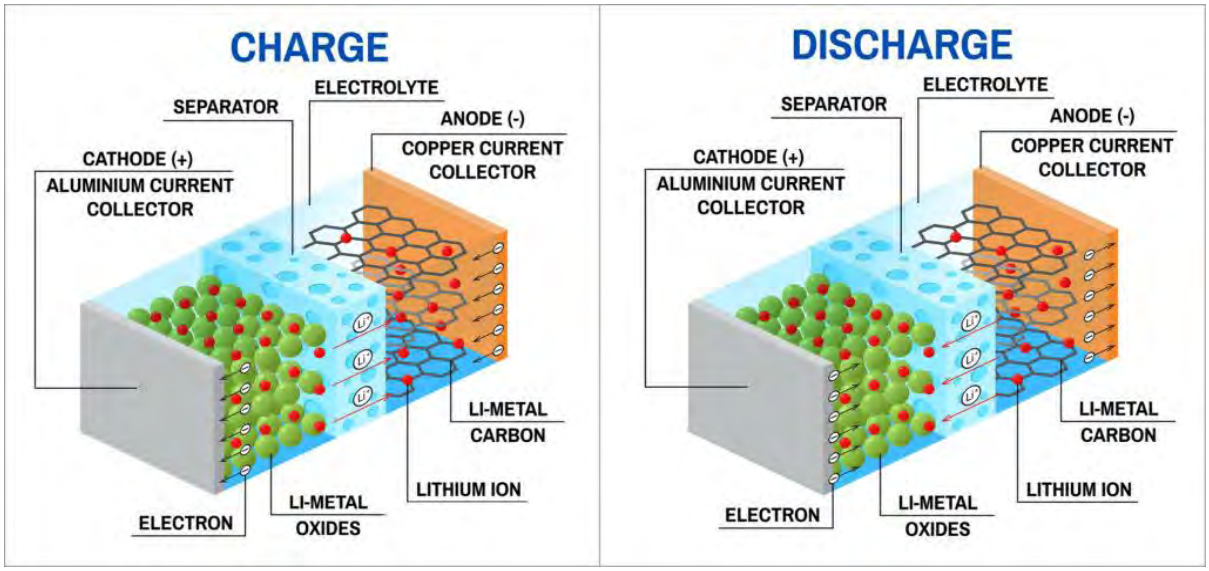

Figure 1.4 working principle of lithium-ion battery [12]

1.6 Cathode materials for Lithium-ion batteries

Goodenough made the initial discovery of (Lithium Iron Phosphate) $LiFePO_4$ with an orthogonal olivine structure as a cathode material for lithium-ion batteries in 1997. The capacity retention of that cathode is 88.8% after 700 cycles at 2C and good cycling properties but not high energy density. Due to their high safety attributes, lengthy cycle life, and thermal stability, (Lithium Iron Phosphate) LFP cathodes have drawn interest [17]. In lithium-ion batteries, $LiCoO_2$ is the most frequently used cathode material. This substance adopts the α-$NaFeO_2$ structure. After 50 cycles, the battery exhibited exceptional capacity retention, maintaining 97% of its initial capacity within the voltage range of 4.4 to 2.75 V. The battery's initial specific capacity was measured at 174 mAh/g. In comparison to $LiCoO_2$, $LiNiO_2$, which also adopts the α-$NaFeO_2$ structure, is more cost-effective and offers a higher energy density (15% by volume and 20% by weight). $LiNiO_2$ displayed the maximum discharge capacity of 200 Ah/kg and voltage range of 3.0 to 4.3V [18].

Cathode material, o-$LiMnO_2$ (orthorhombic lithium manganese oxide), is produced for lithium secondary batteries through both solid-state and sol-gel techniques. (o-$LiMnO_2$) electrodes initial charge curve was characterized by a simple potential plateau at 3.7V [14].

Vanadium oxides as electrode materials is attributed to their ability to create layered compounds. Leaf-like V_2O_5 nanosheets prove to be promising cathode material for lithium-ion battery. Vanadium electrodes function at relatively low voltages, and they have a large capacity

[19]. Phosphates ($LiMPO_4$) possessing the olivine structure (Pnma) present a fascinating family of cathode materials. $LiMnPO_4$ and $LiCoPO_4$ are further phosphates that are utilized as cathodes in lithium-ion batteries. Higher open circuit voltages (4.1 and 4.8 V, respectively) but lower capacities. $LiMn_{1.5}Ni_{0.5}O_4$ has become known as a promising candidate, it has a capacity of about 140mAh/g and operating voltage is 4.7V. Li-O_2, Li-S/C, and Li_2S-Si can provide a significantly higher energy density [20].

Improvements in energy density, longer cycle times, it is necessary for modern lithium-ion batteries. Li ($Ni_{1-x-y}Mn_xCo_y$) O_2 (NMC) oxides, which are layered, are promising cathode materials that have the potential to solve some of the problems with next-generation energy storage devices. Li (Ni, Mn, Co) O_2, offers significant capacity, excellent rate capability, and is capable of operating at high voltages. Nickel in the lithium layer has been found to stabilize the structure during de-lithiation, which enhances cycling performance even if it can be bad for lithium transport. The performance of Li (Ni, Mn, Co) O_2 electrodes is notably improved through over-lithiation, particularly when the cobalt content is low. Although the capacity rises with a higher charging voltage, cycling also causes a faster loss of capacity. Similar to Li ($Ni_{1-x-y}Mn_x Co_{y)}$ O_2, cobalt promotes in the reduction of nickel in the lithium layer and it has been demonstrated that tiny levels of cobalt (up to 0.20-0.25) increase capacity [21].

Table 1.1 Common cathode materials for lithium-ion battery and its properties

Cathode materials	**Typical potential(V)**	**Specific capacity (mAh/g)**	**Specific energy (Wh/kg)**	**Potential window (V)**
$LiCoO_2$	3.9	170	546	2-4
$LiMn_2O_4$	4.0	130	~500	3-4.5
$LiFePO_4$	3.2	140	150-170	2.8-3.6
LiNMC	3.7	250-350	600-760	2.8-4.5
$LiNi_{0.5}Mn_{1.5}O_4$	4.5	147	600	2.5-4

1.7 Next generation cathode materials for Lithium-ion battery

Creation of new cathode materials with improved specific capacity and high running voltage, has been accelerated by the search for high-energy-density lithium-ion batteries [22]. Ohzuku et al., showed NMC111 (also known as NCM 333) capacity of 200Ah/kg between 2.5

and 4.6V or 155Ah/kg if the anodic voltage is restricted to 4.3V. NMC622 and NMC532 are two more types of NMC cathodes material gain a lot of attention. Among the cathode materials used in lithium-ion batteries is NMC532 is a member of the class of $LiNiMnCoO_2$ cathodes and distinguished from other NMC family compositions by its higher energy density and enhanced stability. NMC532 has increased stability, less deterioration, and a longer cycle life and better thermal stability. Although NMC532 offers numerous benefits, but problem of cobalt's sustainability and source reliability. NMC622 gave a discharge capacity of 183mAh/g the usual 1^{st} cycle voltage profile at 0.1 C (1 C=180mA/g). The cathode material NMC811 exhibited the highest discharge capacity among the tested samples, with a remarkable value of 178.93 mAh/g in the charge-discharge measurement results. NMC811 had an ionic conductivity of $1.20x10^{-7}$ S/cm, which was a little bit greater than that of the commercial previous one ($1.04x10^{-7}$ S/cm).

(NMC811) is a common cathode material, researchers are looking towards formulations with more nickel, like NMC622 (6:2:2 ratio) and NMC811 (8:1:1 ratio), to increase energy density. The development of NMC811 with improved stability and lower cost is still being pursued. High energy density NCA-cathodes are currently utilized in electric car applications. In order to improve stability and reduce safety issues associated with high-voltage operation, ongoing research attempts to optimize the composition and surface coatings of these materials. Comparable to other cathode materials (re)insertion, the theoretical specific charge capacity of NCA is 265 mAh/g (0.95 Li+) [23].

Table 1.2 Advance cathode materials for lithium-ions battery and its properties

Cathode materials	**Typical potential(V)**	**Specific capacity (mAh/g)**	**Specific energy (Wh/kg)**
$LiNi_{0.8}Co_{0.1}AlO_2$ [NCA]	3.8	>200	680-750
$LiCoO_2$	3.9	140	546
$LiNi_{1/3}Mn_{1/3}Co_{1/3}O_2$ [NMC333]	3.8	160-170	600-650
$LiNi_{0.8}Mn_{0.1}Co_{0.1}O_2$ [NMC811]	4.8	~200	~700
$LiNi_{0.6}Mn_{0.2}Co_{0.2}O_2$ [NMC622]	4.3	160-190	350

In comparison to the other suggested compounds of that period, it displayed a favorable blend of a relatively higher voltage, approximately 4.7V. Widespread use and commercialization of next-generation cathode materials will be dependent on elements like cost-effectiveness, scalability, and performance enhancements made possible by continuous research and development initiatives. Experts in solid-state chemistry, materials science, electrochemistry, and industrial sectors have dedicated significant attention to these materials as promising contenders for utilization in lithium-ion batteries for electric vehicle (EV) applications [24].

1.8 Lithium nickel manganese cobalt oxide

The NMC (nickel manganese cobalt oxide) cathode material has several different formulations, including NMC811 (nickel-rich cathode materials atomic ratio of $LiNi_{0.8}Mn_{0.1}Co_{0.1}O_2$). It is regarded as a lithium-ion battery's cathode material of the future. NMC811 has a larger nickel content which benefits energy density. It has an atomic composition of 80% nickel, 10% manganese, and 10% cobalt, or 8:1:1. The battery's potential energy density improved by the larger nickel content, which helps to boost specific capacity and higher voltage operation. NMC811 produce a high specific capacity of about 200mAh/g with a relatively high average discharge potential of 3.8V against Li+/Li. Its capacity between

3-4.3V is (1C=180mAh/g). The electrochemical capabilities of the NMC811 were evaluated at 0.1C rate (1C= 275mAh/g) and 4.5V vs. Li/Li+. The lithium positive ion intercalation routes will be wider as the crystal grows in size, increasing the storage capacity as a result. As compared to other conventional NMC formulations like NMC111 or NMC622, NMC811 has a higher energy density. Increased power potential of NMC811 is a result of its high nickel content. Faster rates of charging and discharging make it appropriate for high power output applications like electric vehicles. Cathode materials must prioritize safety. Compared to certain other high-nickel content cathode materials, NMC811 demonstrates higher thermal stability and a lower danger of thermal runaway. NMC811 have showed enhanced cycle life, indicating superior long-term stability and durability. Limited surface area and superior mechanical stability allows them to offer higher volumetric energy density and high gravimetric energy density [25].

To successfully commercialize NMC811 cathodes, several problems still need to be solved, prominent among them being their noticeably quicker voltage and capacity fading when compared to NMC materials with lower nickel concentrations. Few problems with this cathode materials like, nickel cations block lithium-ion diffusion channels as a result defects produce in structure which causes cycled NMC811 to have slow kinetics and poor rate capability. Material frequently exhibits an unstable cycle life performance because of the numerous phase changes that take place during charge and discharge cycles. Capacity fading and a gradient in nickel content of the cycling sample happened when nickel ions diffuse fast in electrolyte [26].

Divalent and insulating NiO phase can be formed on the surface by effectively reducing the significant concentration of unstable Ni^{4+} in the de-lithiated state (H-3 phase). Reduction of unstable Ni^{4+} helps mitigate capacity fading issues that can occur during cycling [27]. Coating layer significantly improves NMC811 materials' overall electrochemical performance, and in particular, results in better reversible capacity and a notable improvement in capacity retention [28]. To increase performance and economic viability of NMC811 cathode materials in lithium-ion batteries, researchers are actively trying to optimize synthesis processes, surface coatings, doping and overall composition [29].

1.9 Problems with Lithium nickel manganese cobalt oxide

NMC811's instability at high voltages, which can cause side reactions and deteriorate battery performance, is one of its main drawbacks. Because of the increased valence of the surface nickel towards the highly reactive Ni^{4+} and the bulk migration of Ni^{2+} into the lithium-layer, the increased nickel content may lead to enhanced cation mixing and parasitic reactions. Since performance deterioration is substantially worse when cells are charged over 4.2V compared to Li^{+}/Li. Slow Li^{+} diffusion results in the accumulation of overpotentials, which reduces the cathode material's utilization and capacity. Although there are issues with oxygen release, when Li+ is inserted or removed during charge or discharge, crystal lattices (primary particles) expand and shrink, which gradually creates strain and causes secondary particles to shatter. Intergranular/intragranular cracking, and surface phase reconstruction, nickel-rich cathodes continue to experience quick capacity fading and voltage dropping challenges. Transition metal dissolution may threaten anodes through electrode position, solvent reduction catalysis and all of which can obstruct lithium intercalation and lower capacity. Galvanostatic intermittent titration method (GITT) measurements show that Li^{+} diffusivity went up as the nickel content increased. 10^{-12} to $10^{-13} m^2/s$ chemical diffusion coefficient ranges for NMC811 [30]. Researchers want to boost lithium-ion battery capacity and energy density while retaining high cycling stability and reducing safety issues by boosting the nickel content.

1.10 Strategies to solve NMC811 problems

To enhance its performance and safety, (NMC811) must overcome a number of obstacles and problems. To prevent obstructing lithium-ion diffusion and raise resistance at the electrode/electrolyte interface, cover the electrode surface with a homogeneous layer of controlled thickness. A coating that has a huge covering area, a high electron throughput, is pinhole-free, and is extremely conformal for secure positive delay transition metal dissolution at the electrode-electrolyte contact. Morphologies of coatings produced by various surface modification techniques may differ greatly, directly affecting the positive electrode characteristics and electrochemical performances [31].

A large number of oxides, phosphates, fluorides, composites, including lithium, and carbon-based compounds are frequently utilised as coatings for positive electrode modifications. Al_2O_3, ZrO_2, V_2O_5, MgO, ZnO, and TiO_2 are just a few of the metal oxide coatings that have been claimed to improve cycle performance and rate capability [19]. As a result, coated NMC provides a longer lifespan at low C-rates, but MgO coated NMC gives better capacity and energy at higher C-rate. Tungsten oxide, in contrast, has strong conductivity and can be employed as a coating on nickel-rich electrode. Additionally, WO_3 and lithium have a reaction that aids in the removal of certain lithium traces from the surface of NMC materials. Various coatings can improve NMC's electrochemical and structural stability in various ways [20]. Rate performance, long cycling performance, and high voltage performance better when (NMC811) coated with carbon [32].

The cycling stability, voltage stability, and safety of the battery can all be enhanced by adjusting the composition and concentration of electrolyte salts and solvents. With sulfone-based localised high-concentration electrolyte, lithium metal battery cycle performance has been greatly enhanced [24]. Some of the problems with the NMC811 material can be solved by changing its shape and composition. The stability, cycling life of NMC811 cathodes, specific capacity, are being improved by methods as doping with additional elements, regulating particle size and shape, and optimising the crystal structure. Li-O used in lithium-ion battery electrodes, especially high concentrated nickel material (NMC), can be modified through doping. To increase the cycle stability of NMC811 zirconium (Zr) and aluminium (Al) as complementary coating and doping materials, compared their qualities, and then logically integrated their advantages [33]. Layered lithiated nickel-rich oxides can be stabilized by doping and/or coating, which has been demonstrated to produce great stability and long-term cyclability [34].

The structural stability is increased by the Tungsten (W) and Ca^+ substitution. The partial Mo^{6+} doping and Sn-doped materials increases the samples' thermal stability and lowers the total heat generated during chemical reactions in a nickel-rich material [17]. During Li+ intercalation and deintercalation, the Li-ion site doped sodium-ion can act as barrier-ions to keep the positive electrode materials' structural stability [35].

Battery designs that use NMC811 cathodes can be made to perform better overall and be safer by optimising the cell design and manufacturing procedures. This covers elements like electrode density, porosity, binder type, and thickness. Better performance and consistency of

NMC811-based batteries may result from improving the uniformity and stability of electrode manufacturing processes. NMC811 can be modified or combined with other cathode materials to improve overall performance and safety. To increase performance, safety, longevity of lithium-ion batteries, new methods and ideas are always being researched in the quickly growing field of battery technology.

1.11 MXene

MXenes, are 2D transition metal carbides and/or nitrides exhibiting unique physiochemical traits. They are renowned for having exceptional mechanical and electrical conductivities. Because of its excellent electronic conductivity, great mechanical strength, and abundance of functional groups, MXene stands out among them as a useful coating material. When the A-site element is selectively etched from MAX phase precursors, a class of two-dimensional transition metal carbides and carbonitrides is created. These compounds have potential for usage in energy storage applications. MXenes have generic formula $M_{n+1}X_nT_x$ (n = 1, 2, 3, or 4), where M is one or more transition metals, X is carbon and/or nitrogen, and T_x is the surface terminations (-OH, -O, -F, -Cl, etc.). The process of creating MXene involves selectively etching the appropriate MAX phase's A-layer in F-containing solutions like HF or a LiF+HCl solution. There have been reported HF-free techniques such electrochemical etching, molten salt etching, and hydrothermal approaches, however these take hours to days to create MXenes [25]. Conductivity of MXenes can span a wide range, from values below 1 S/cm to several thousand S/cm. This variation is heavily influenced by factors such as the specific synthesis techniques employed and the methods used for their delamination. For example, the conductivity of HF-etched $Ti_3C_2T_x$ is relatively low at 2 S/cm. The conductivity of LiF + HCl-etched $Ti_3C_2T_x$ can be significantly higher, reaching up to 1500 S/cm. This substantial contrast in conductivity due to differences in defect density and F-terminations. Delamination of LiF + HCl-etched $Ti_3C_2T_x$ lead to further enhancements in its conductivity [36].

The $M_{n+1}AX_n$, general formula describes the stacked hexagonal carbides and nitrides that make up the MAX-Phases, where M are transition metals (Ti, V, Nb), A are group III-A (mostly Al,) elements and X are carbides, nitrides are carbonitrides. MAX-Phase uses for making MXene in which A-layer etched by different synthesis routes. Prepared MAX-Phases are titanium aluminium carbide (211), titanium aluminium carbide (312), similarly vanadium aluminium carbide (211), vanadium aluminium carbide (312) etc. Developing etching techniques, including as alkali etching, in situ HF-forming etching, electrochemical etching,

molten salt etching, and delamination procedures are some examples of etching processes. Easy and non-hazardous method is molten salt etching. The majority of Al-containing MAX phases can be processed using aqueous etching techniques at low operating temperatures to create hydrophilic MXenes [36].

1.12 NMC811 MXene-based cathode composites

Composite cathodes based on NMC811 MXene are the recently developments used in lithium-ion battery. MXene family includes two-dimensional carbonitrides, nitrides, and carbides of transition metals, they are renowned for having exceptional mechanical and electrical conductivities. Because of its excellent electronic conductivity, great mechanical strength, and abundance of functional groups, MXene stands out among them as a useful coating material. MXenes can be mixed with other substances to improve their applications-specific characteristics. They have layered structure. MXene components are included into the NMC811 cathode structure in the case of MXene-based composite cathodes. The cathode's overall performance and stability are designed to be enhanced by this combination [37].

NMC811 cathode could get a number of advantages when coated by MXene. High electrical conductivity in MXene materials can increase the battery's rate of charge and discharge, mechanical stability and strength, which may reduce the chance of the cathode's structural breakdown during cycling. MXene can be added to the composite cathode to increase the (LIBs) overall performance, energy density, and cycle life [38].

A multipurpose addition called few-layer and rod-like MXene ($Ti_3C_2T_x$) considerably improves the mechanical properties, cycle performance, and rate capability of Li/NCM811 cells. NCM811 containing 2.5 weight percent coated on MXene offers best rate performance with a high discharge capacity of 209mAh/g at 0.2C high reversible capacity of 95mAh/g at 8C. In comparison to the pure NCM811, which contains no MXene (0-MXene), 2.5-MXene may retain capacity up to 77.0% after 100 cycles at a rate of 0.5C. Exceptional results are attributable to the efficient and multipurpose inclusion of MXene facilitates the formation of a flexible conductive network, enabling the storage and release of Li+ ions through cation intercalation, thereby offering a larger space for deformation., to provide a cathode electrolyte interface layer that is physically protective, and to prevent the M←→H2 phase change for $LiNi_{0.8}Mn_{0.1}Co_{0.1}O_2$ cathode [39].

To improve the electrochemistry of the nickel-rich $LiNi_{0.8}Co_{0.1}Mn_{0.1}O_2$ (NCM811) cathode or any other cathode materials, coating with MXene significantly enhance electrochemical characteristics of that cathodes. The (Li/NCM811) cell maintains a 166.2 mAh/g capacity after 100 times charge/discharge of 0.5C current density cycling, with a retention rate of 90.7%. The method of coating commercial PP with MXene is considered a direct, effective, and successful strategy for augmenting the electrochemical capabilities of the nickel-rich NCM811 cathode. This method finds widespread application in high-performance lithium-ion batteries [40].

Chapter No. 2

Literature Review

In this chapter we have discussed a concise overview of literature related to (NMC) cathode materials and nickel-rich cathode materials within the context of lithium-ion batteries in which their synthesis method, advantages, drawbacks and their solution are discussed. After that we have discussed MXene ($Ti_3C_2T_x$), its synthesis, properties and MXene based composite.

Introduction

Transition metal oxides layered structured, using the general formula $LiNi_xCo_yMn_zO_2$, often known as NMCs, is crucial cathode material for lithium-ion battery. Lithium-ion batteries are being developed with greater energy density. Nickel-rich cathode materials are a good choice because they are renowned to be the strongest candidates for lithium-ion battery. It is a tool to produce batteries with high energy density. Nickel-rich substances have been formulated as the next-generation cathode materials for use in commercial lithium-ion batteries designed for automotive applications, expressing significantly improved energy density. NMC811 has proved to be good cathode materials because of its high energy density that is around (200mAh/g). Similarly, NCA811 replaces aluminium with manganese as a high capacity and high energy density cathode material). The physicochemical qualities (volume expansion, chemical stability, excess lithium, Li+ diffusivity and electrical conductivity) and the microstructure (particle shape and surface/bulk structural stability) of nickel-rich materials affect their electrochemical properties and safety. This has been proposed that high manganese (Mn) concentration provides thermal stability. While high content of nickel (Ni) provides good discharge capacity [41].

In contrast, these cathode materials encounter problems when coprecipitation method use for synthesizing NMC is the cause of structure cracking, such as battery performance (capacity fading) due to lithium plating caused by electrolyte side reactions. Capacity loss occurs when LiOH reacts with $LiPF_6$ to begin producing HF, which is the consequence of (transition metal) dissolution. Transition metal dissolution disturb solid electrolyte surface on graphite surface, this will result of loss capacity and short life cycle of lithium-ion batteries (NMC). To solve this issue, cathode of the (NMC811) is coated with a hybrid of lithium metal oxide ($LiAlO_2$) and superconductor ($LiTi_2O_4$,) which improves the electronic conductivity of the (NMC811). This method is applied on all nickel-rich cathode materials to optimize battery

performance. Scientists use different strategies like ion doping, surface coating and lithium salts for improving the cycling stability of nickel-rich cathode materials. (NCA811) and (NMC811) lithium-ion batteries have fault rapid discharge and a higher nickel composition, which results in more capacity but lower cycling and thermal stability. Cobalt helps to reduce cationic disorder, whereas manganese helps to maintain the structure [46].

NMC cathode materials have been synthesized using variety of techniques, which encompass the hydrothermal approach, combustion process, co-precipitation, solid-phase synthesis, and sol-gel method, among others. Synthesis procedure has a direct impact on the morphological structure, crystallinity, particle size, and electrochemical performance of NMC cathode materials. The co-precipitation method stands out as a widely employed strategy for fabricating precursor materials intended for the cathodes of lithium-ion batteries. Due to its simplicity, scalability, and capacity to create a homogenous structure at the particle size, co-precipitation technique is beneficial in the ability to employ a variety of raw materials, including sulphates, chlorides, organic anions, and nitrate salt to makes battery sector particularly advantageous. Diminished particle size commonly improves the facilitation of Li+ ion integration and extraction. This outcome stems from an enlarged interface area connecting the active material and electrolyte, alongside diminished ion diffusion pathways within the solid phase while undergoing charge and discharge sequences [41].

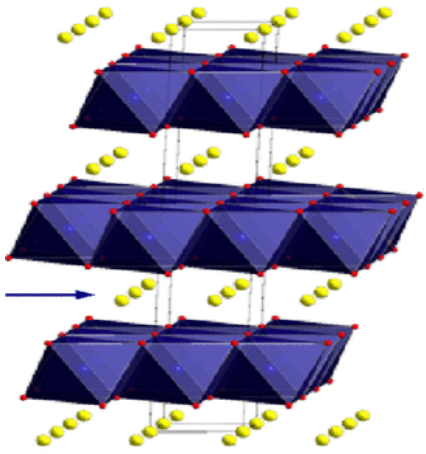

Figure 2.1 The ideal NMC has an R-3m structure with transition metal [41].

Layered cathode material $LiNi_{1/3}Mn_{1/3}Co_{1/3}O_2$ (NMC333) was created using a self-combustion process utilizing sucrose as the fuel and lithium, nickel, manganese, and cobalt nitrates as the precursors [41]. Ryu et al., 2013 urea-assisted solvo/hydrothermal technique for the synthesis of dumbbell-like $LiNi_{1/3}Mn_{1/3}Co_{1/3}O_2$ precursors combined with nano cubes.

Consistently shaped particles exhibiting higher tap density (1.23 g/cm³) and superior capacity retention post 50 cycles (96.5%) compared to corresponding substances synthesized at pH 11.4 (with a median particle size of 16 micrometers). NMC333 structure, which mostly displays Mn, Ni, and Co in Mn^{4+}, Ni^{2+}, and Co^{3+} states that are most stable structure. Two of the most efficient methods are surface coating and lattice doping to further stabilize the cathode structure and improve its electron conduction capabilities [42].

Cathode material $Li_xNi_{0.4}Mn_{0.3}Co_{0.3}O_2$ are layers of transition metal oxides are often referred to as (NMC433). Precursor preparation $NMC433(OH)_2$ with ratio of 40% nickel, 30% cobalt, and 30% manganese is prepared by co-precipitation, solid state or sol-gel method. Homogeneity and the right distribution of the constituents, precursor materials are carefully combined and milled. This process aids in creating a homogeneous composition in the finished (NMC433) products. Lithium ions create the desirable (NMC433) structure by substituting lithium-ions for some transition metal ions in the crystal lattice. Its show 160mAh/g between 3.0 to 4.3V [43].

Among the cathode materials used in lithium-ion batteries is (NMC532), is distinguished from other NMC family compositions by its higher energy density and enhanced stability. Great energy storage and delivery capability of (NMC532) materials makes them appropriate for applications requiring long-lasting power. (NMC532) has increased stability, less deterioration, and a longer cycle life than prior (NMC433) formulations. (NMC532) cathodes offer better thermal stability because of its high-power output and energy density it is often used in electric cars (EVs) and (HEVs). Cathode material tend to have a relatively high capacity, often around 160-170 mAh/g making them capable of storing a significant amount of energy per unit mass. It also has some drawbacks like the material is more expensive than other cathode materials, and there are some questions about the cobalt's sustainability and source reliability [43].

Qian et al., 2020 reported (SC-NMC) materials can be created by molten salt. Liang et al., $NMC622(OH)_2$, produced through co-precipitation, exhibited greater sphericity when synthesized at pH 11.2, along with an increased tap density measuring 1.65 g/cm³ [44]. At a temperature of 900°C, particles of $[Ni_{0.6}Mn_{0.2}Co_{0.2}(OH)_2]$ hydroxide precursor, known as SC-NMC622, were generated using LiOH and a touch of Li_2SO_4. The combination of LiOH and Li_2SO_4 creates a molten salt mixture at the specified temperature. Galvanostatic cycling experiments in the voltage range (2.8-4.3V), (SC-NMC622) gave a discharge capacity of 183 mAh/g better than that of the polycrystalline (NMC622) 178 mAh/g at 0.1C [45].

Wijareni et al., 2022 using two separate nickel sources, mixed nickel-cobalt hydroxide precipitate (MHP) and nickel sulphate, cathode precursors of $NMC811(OH)_2$ were created by the coprecipitation approach. Synthesized precursors' elemental analysis found Ni: Mn: Co mol ratios of 0.8:0.08:0.12 in the precursors. According to the examination of particle sizes, the largest average particle size was found in (NMC811) 285.2 microns. The battery cylindrical cells using (NMC811) as the cathode material demonstrated 178.93mAh/g the best charge-discharge value this agrees with the findings of the electrochemical impedance measurements, which revealed the highest ion conductivity. NMC811 had an ionic conductivity of $1.20x10^{-7}$ S/cm [42].

Thomas et al., 2022 reported the Ni^{2+} ion's susceptibility to oxidation during synthesis makes it difficult to manufacture nickel-rich cathode materials like (NMC811), careful control of the synthesis conditions is necessary. Advantageous for the creation of the precursor NMC hydroxide ($Ni_xMn_yCo_z$ $(OH)_2$) which is often combined with a lithium salt and calcined to generate $LiNi_xMn_yCo_zO_2$ with a layered α-$NaFeO_2$ crystalline structure. Van Bommel et al., illustrate when $NMC811(OH)_2$ particles were synthesized under pH 11.5 conditions, in contrast to particles produced at pH 11.8. The former exhibited a nearly uniform size and a heightened tap density of 1.91 g/cm³, surpassing the tap density of the $Ni_{0.33}Mn_{0.33}Co_{0.33}(OH)_2$ precursor at 1.5 g/cm³ [46].

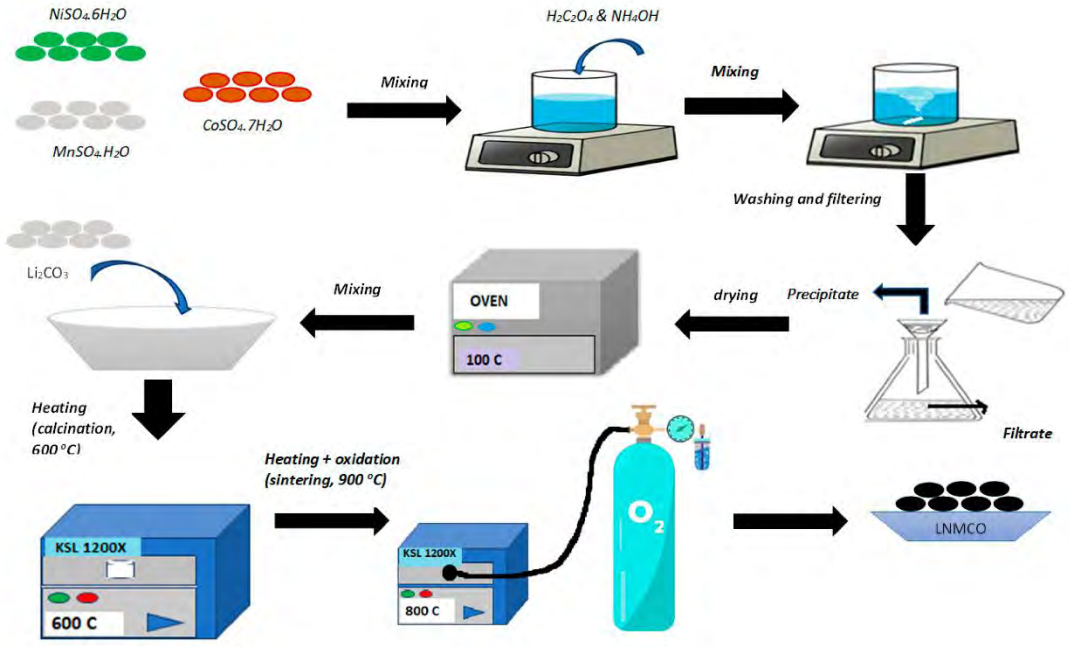

Figure 2.2 Preparation steps for NMC cathode materials via co-precipitation method [46].

Problems and its solution

S Zhang et al., 2019 reported $LiNi_xCo_yMn_zO_2$ (NCM) and $LiNi_xCo_yAl_zO_2$ (NCA), two nickel-rich layered oxides with x+y+z= 1 and x>0.8 respectively, best options for the cathode material of high-energy lithium-ion battery. The two fundamental issues of (1) performance deterioration and (2) safety danger throughout the course of the battery's lifetime, however, restrict their use in practical lithium-ion batteries. Swelling and impedance growth, as well as operational voltage and battery capacity reductions, are all signs of performance deterioration. Safety issue (thermal runaway), which happens when abuse situations like overcharging, overheating, and electric shorting are present, poses a safety risk. Battery volume and impedance rise along with a decrease in capacity and operational voltage as performance degrades. Under abusive situations like overcharging, overheating, and electric shorting, the risk of thermal runaway increases [47].

R Jung et al., 2019 reported specific capacity rises as nickel concentration rises, while thermal stability and capacity retention decrease. Multiple phase changes occur during the charging process, from hexagonal (H1) to monoclinic (M) to hexagonal (H2 and H3) phases, and the discharging process then reverses these phases. It is discovered that although the potential for H2 to H3 phase transitions reduces as the nickel concentration rises, the potentials for H1 to M and M to H2 phase transitions are not significantly different. For NCM622, NCM523, and NCM333, the H2–H3 phase transition occurs at >4.6V vs. Li^+/Li, whereas it happens at 4.3V and 4.2V for those with x=0.8 and 0.9 [48].

Presence of residual lithium compounds (RLCs); and oxygen loss, particularly as a result of the H3 phase's thermodynamic instability. Nickel-rich layered oxides will always include residual lithium compounds and number of these compounds rises with the nickel concentration. RLCs are initially present as Li_2O and during storage, interactions with the surrounding air's H_2O and CO_2 cause lithium to ultimately transform into LiOH and Li_2CO_3.

Han et al., 2011 reported washing with water or an acidic solution as a result of residual lithium compound removed. Residual lithium compounds also removed by surface coating process since the coating solution is often an acidic aqueous solution as a result of the hydrolysis of the coating precursors i.e., the metal ions of salts and halides. Heating at a high temperature may be used to eliminate the residual lithium compounds on the surface [49].

When Ni^+/Li^+ is mixed, both the capacity and the mobility of lithium are decreased, and crystal structure changes from layered over spinel to a rock-salt phase that resembles NiO.

Ni/Li mixing is a problem with the thermodynamic instability of layered oxides rich in nickel. P. Kalyani et al., 2005 addressed the solution of Ni^{+}/Li^{+} mixing, it can be prevented by reducing nickel content and restricting SOC, but doing so comes at the penalty of material cost and capacity. It has been shown that restricting Ni^{+}/Li^{+} mixing in the synthesis may be achieved by adding excessive amounts of lithium sources and raising oxygen partial pressure as it moves towards the layered oxide product [50].

Q Xie et al., 2019 added former provides safeguarding the de-lithiated cathode against undesired interactions with electrolyte components, while the latter contributes to the chemical stabilization of the layer structure. Both the lithium and nickel sites are open to cation entry for cation doping. Cations with lower valence, such as Mg+ and K+, are primarily introduced into the lithium sites through a preference for the same principle underlying M/Li mixing [51].

F Kong et al., 2019 investigated that all layered oxide cathodes show oxygen evolution at the end of charge, and the start potential of oxygen evolution decreases as the nickel content rises. All layered oxides were found to exhibit the oxygen evolution reaction (OER), which is caused by the thermodynamic instability of the H-3 phase. Chemical stabilization of NiO bonds by cation doping is the most practical solution for oxygen evolution reaction [52].

According to Park et al., there is obvious microcracking in the voltage areas over 4.0V because the H2 to H3 phase shift is perfectly timed with the lattice unit cell volume change and secondary particle structure breakdown. When lithium is inserted into or extracted from a material, more phase transitions and higher volume changes occur, which will further induce fractures within the secondary particle along the grain boundary. When this occurs after multiple charge/discharge cycles, the structural stability suffers. These cracks become greater as the temperature, operating voltage, and nickel content rise. Single crystal (NCM) material has some improved strength and particle crack-reduction qualities, as well as higher pellet density and volumetric energy density. Long-term cycles have not damaged a single crystal particle's integrity [53].

Utilizing a transition metal featuring a higher oxidation state, the nickel-rich (NMC) material provides an increased charging capacity. Metal tends to emit active oxygen, which causes an electrolyte-cathode side reaction. The cathode and electrolyte will experience a more intense side redox reaction when thermal storage and cycling take place at a high temperature. Lithium cells made from nickel-rich NMC-materials are thus faced with significant issues in cycling, thermal storage, and safety. Fundamentally, the precursor $NMC(OH)_2$ determines how

well NMC-material performs. Preparing NMC-materials benefits naturally from a well-crystallized precursor with improved texture, fewer surface flaws, and reduced impurities. In industrial settings, precursor material is produced in large quantities using a continuous stirred tank reactor (CSTR). Sintering is a key factor in NMC-materials' performance; excessive or inadequate sintering will lead to subpar electrochemical performance. For best results, big and tiny particles should be sintered at various temperatures. Regarding electrochemical performance, it might be said that batch-produced precursors with a respectable level of uniformity are favored for NMC-materials [54].

Wilcox et al., 2009 reported that modifying functional materials often involves doping. In comparison to pure $LiNiO_2$, $LiNi_{1-x-y}Co_xMn_yO_2$ is a mutually doped solid solution made up of the elements $LiNiO_2$, $LiCoO_2$, and $LiMnO_2$. It exhibits greater electrochemical and thermal stability. Mg, Al, Fe, Ti, Zr, Cr, Y, Ga, etc elements are selected for doping for stabilize the structure of the NMC-materials [55].

Since the dopants increased the lithium slab distance, they were able to promote the transport of lithium ions. Aluminum doping increases the (NMC) cathode material's cycle stability and thermal storage at the expense of capacity and rate capability. Incorporating titanium through doping proves advantageous in enhancing cycle durability and rate capability. Similarly, substituting chromium for manganese and aluminum for nickel leads to an enhancement in both cycle performance and rate capability. The improved lattice parameter "c" in doped materials facilitates the diffusion of lithium ions, further contributing to these benefits. Mg and F are co-doped to decrease cation mixing and enhance the material's capacity, cycle performance. Another efficient method for improving the stability of nickel-rich cathode materials is surface coating reported by Bai et al., 2013. Surface has been coated with one or more metal oxides or phosphates that are nanosized, such as Al_2O_3, TiO_2, CeO_2, Y_2O_3, ZrO_2, and MPO_4 (M = Al, Fe). Surface coating has the following effects (1) partial removal of the oxidizing cathode from the electrolyte solution; (2) scavenging of the harmful HF species from cathode materials under attack; and (3) consumption of the surface impurities in lithium (4) Surface doping boost brought on by a coating element's high concentration diffusing into the thin surface layer [56].

Chen et al., 2019 discuss increasing manganese content and reducing cobalt content, leads to increase the thermal stability of (NMC) with a specific level of nickel content. To enhance thermal stability, it is recommended to increase particle sizes and reduce the specific

surface area of the cathode material. To minimize the "thermal runaway" of lithium-ion batteries, which is caused by the de-lithiated cathode material's exothermic reaction, appropriate doping and coating strategies [54].

Lipson et al., 2021 discuss thermal stability and cycling performance increased by coatings. Wang et al., 2020 reported hybrid coating layer of ($LiAlO_2$) on nickel-rich cathode material enhance it cycling. ($LiAlO_2$) is an excellent ionic conductor because the structural deterioration of the coating layer and the occurrence of fractures may be reduced during prolonged cycling. NMC622 material exhibit 166.8 mAh/g of discharge capacity and 74.5% of capacity retention at 5C after 300 cycles after hybrid coating [54].

Outlook

The industry has steadily migrated away from $LiNi_{0.3}Mn_{0.3}Co_{0.3}O_2$ in order to enhance the nickel content in $LiNi_{1-y-z}Mn_yCo_zO_2$ as a result of the growing interest in lithium-ion nickel, cobalt, and manganese oxide batteries. High nickel content has the potential to enhance volumetric energy density, and capacity for nickel concentration below 0.5. However, (NMC-622) to (NMC-811)'s high nickel concentration causes issues and reduces lithium-ion batteries capacity. NCA capacity decreases to 180mAh/g. Doping various elements into materials for nickel-rich cathodes is the solution to this problem.

MXene ($Ti_3C_2T_x$) and its synthesis

By selectively etching the A-layers from MAX phases, MXenes have been created. General formula of MAX-Phase $M_{n+1}AX_n$, M is an early transition metal, A is an element from group IIIA or IVA, X is an element from group IIIB or IVA, and n is either 1, 2, or 3. There are presently more over 70 MAX phases and many more solid solutions of these phases known. oxidation-sensitive materials, including as porous Ti, Ti_3SiC_2, and Ti_2AlN MAX-phases, in an air environment, created by the molten salt-shielded synthesis (MS^3) technique in 2019. Layered hexagonal crystals ($P6_3/mmc$ symmetry) make up the structure of these materials. If neighboring $M_{n+1}X_n$ layers are interspersed with pure A-layers, M layers are almost completely closed packed, and X atoms occupy the octahedral positions. Because M-X bond is typically mixed covalent/metallic in MAX phases but metallic in M-A connections, the bonds between MAX layers are difficult to break mechanically. Although aqueous acidic solution produce carbide and carbonitride MXenes effectively, they are unable to etch away A-layers from nitride-based MAX phases for unknown reasons. Over their carbide relatives, nitride-MXenes may provide a number of benefits. The electronic conductivities of transition metal nitrides are

known to be greater than those of carbides. MXenes are chemically unstable, especially at high temperatures, due to MAX-Phase oxidation sensitivity. Ti-N is a well-known potential plasmonic material, therefore nitride MXenes will perform better in transformation optics and metamaterial devices [25].

Patrick et al., reported first two-dimensional transition metal nitride, Ti_4N_3-based MXene, was synthesized and published. Utilizing density functional theory calculations, researchers examined both unmodified Ti_4N_3 and $Ti_4N_3T_x$ with terminal groups, revealing the most energetically stable configuration for this MXene compound. It is expected that Ti_4N_3 will be metallic both bare and functionalized [57]. MXenes, such as Ti_2CT_x, Cr_2CT_x, and V_2CT_x, is accomplished using a general method based on thermally assisted electro chemical-etching. Ti_2CT_x is created a two-stage process during the etching of Ti_2AlC with Cl etchant. An applied voltage initially eliminates aluminum atoms from stacked carbides at stage 1 because the Ti-Al link is weaker than the Ti-C bond, after which step two involves the etching of both aluminum and titanium atoms until only single layer carbon atoms are left. E-etching procedure, the atomic percentage of the aluminum element significantly decreased (from 11.74% to 0.69%), indicating that aluminum atoms were successfully removed from Ti_2AlC. E-etching process become more versatile, effective, and safe way to synthesize a variety of MXene compounds on a big scale as compared to HF method [58].

Tengfei et al., used HF-routes for preparing two-dimensional MXene. Most synthesis use HF, which is very corrosive and bad for lithium-ion batteries. This technique was modelled after bayer process used in the refinement of bauxite. Fluorine-free technique produces multilayer $Ti_3C_2T_x$ with 92 weight percent concentrated. The main determinant of $Ti_3C_2T_x$ production is temperature, while the concentration of NaOH has an impact on the purity of the resultant MXene. Sin et al., 2019 reported two-dimensional MXenes made by HF-acid etching. More than 20 reported MXene synthesizes using HF-related techniques [59].

First time in 2019, carbide MXenes created directly from elemental precursors using molten salts (lewis salt etching). To achieve a low-melting-point effect, a protective layer of molten salt is generated around the sample under low temperatures. KBr serves as a reaction medium, shielding products from oxidation while undergoing high-temperature synthesis. Employing M, A, and X (carbon) atoms as precursors, one-pot molten salt synthesis to produce MXenes. Chen et al., 2021 prepared (MXene) $Ti_3C_2T_x$ by molten salts method [11].

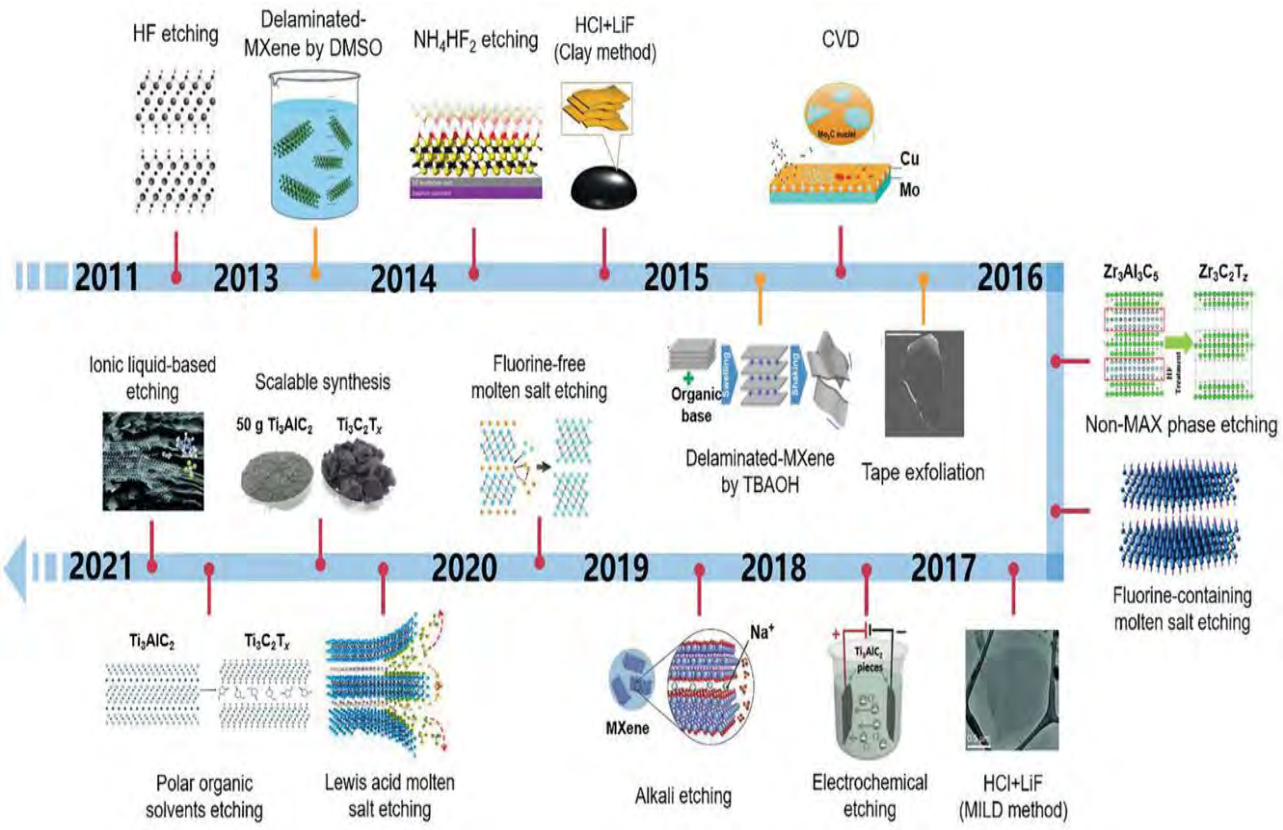

Figure 2.3 Timeline of the progress in MXene synthesis [36]

Table 2.1. Summary for synthesis of MXene [60]

Precursor	MXene	Etchant	Temp	Time	Yield
Ti_2AlC	Ti_2CT_x	HF	25°C	10h	80(%)
V_2AlC	V_2CT_x	HF	25°C	90h	60(%)
Nb_2AlC	Nb_2CT_x	HF	25°C	90h	100(%)
Ti_2AlN	Ti_2NT_x	HF	25°C	24h	NA
Mo_2Ga_2C	Mo_2CT_x	HF	50°C	3h	NA
$(Ti_{0.5}Nb_{0.5})_2AlC$	$(Ti_{0.5}Nb_{0.5})_2CT_x$	HF	25°C	28h	80(%)
Ti_3AlC_2	$Ti_3C_2T_x$	HF	25°C	2h	100(%)
$(V_{0.5}Cr_{0.5})_3AlC_2$	$(V_{0.5}Cr_{0.5})_3C_2T_x$	HF	25°C	69h	NA
Ta_4AlC_3	$Ta_4C_3T_x$	HF	25°C	72h	90(%)
Nb_4AlC_3	$Nb_4C_3T_x$	HF	25°C	96h	77(%)
V_4AlC_3	$V_4C_3T_x$	HF	25°C	165h	NA
Ti_3AlCN	Ti_3CNT_x	HF	25°C	18h	80(%)
Mo_2TiAlC_2	$Mo_2TiC_2T_x$	HF	25 °C	48h	100(%)
V_2AlC	V_2CT_x	LiF+ HCl	90 °C	48h	NA
Ti_3AlC_2	$Ti_3C_2T_x$	LiF+ HCl	40 °C	45 h	100(%)
Ti_3AlCN	Ti_3CNT_x	LiF+ HCl	35 °C	12 h	NA
Cr_2TiAlC_2	$Cr_2TiC_2T_x$	LiF+ HCl	55 °C	42 h	80(%)

MXene and MXene based composites

MXenes are recognized as promising candidates for the synthesis of multifunctional composites due to their two-dimensional form, layered structures, and high degree of flexibility, which has inspired a rush in research into MXene-based composites. MXenes possessing exceptional mechanical attributes, hydrophilic surfaces, and metallic conductivity, have the potential to augment the mechanical and thermal properties of polymers through their incorporation into polymer composites [60].

According to Ling et al., a mono-layered composite of MXene and polyvinyl alcohol (PVA) was created by combining an aqueous solution of PVA with a colloidal solution of

$Ti_3C_2T_x$ films. PVA is dispersed between layers of $Ti_3C_2T_x$ in the $Ti_3C_2T_x$-PVA composite. It has a high thermostability because $Ti_3C_2T_x$, and extremely hydrophilic PVA may form robust hydrogen bonds. $Ti_3C_2T_x$-PVA as compared to independently $Ti_3C_2T_x$ with PVA, gives greater flexibility, tensile strength, and compressive strength. Having a high conductivity, $Ti_3C_2T_x$ gives this composite [61].

Polyacrylamide (PAM) and $Ti_3C_2T_x$ are combined to create a composite by Naguib. The composite offers the finest mechanical characteristics and maximum electrical conductivity of $3.3x10^{-2}$S/m at 6 weight percent $Ti_3C_2T_x$. Alginate/PEO, poly (ethylene-oxide), poly(vinylpyrrolidone), and poly (acrylic-acid) also combined with MXenes to make composites. Additionally, a lot of them exhibit strong electric conductivity, making them intriguing for use in wearable electronic devices [62]. MXene-oxide composites, exhibit higher electrical conductivity and remarkable electrochemical durability. Consequently, they hold promise as electrode materials for applications like lithium-ion or sodium-ion batteries, in addition to supercapacitors. TiO_2- $Ti_3C_2T_x$ nanocomposites created hydrothermally by Zhu et al., and used as electrodes in electrochemical supercapacitors. An electrode made of synthetic TiO_2-$Ti_3C_2T_x$ has a high specific capacitance and great cycle stability. TiO_2-$Ti_3C_2T_x$ electrode illustrate outstanding electrochemical performance [37].

Zhang et al., manufacture layered orthorhombic Nb_2O_5-$Nb_4C_3T_x$ hierarchical composite. Nb_2O_5 is consistently distributed throughout the $Nb_4C_3T_x$ sheets in the Nb_2O_5-$Nb_4C_3T_x$ composite, reducing the length of the ion diffusion routes. TiO_2, Nb_2O_5, Li_4 Ti_5 O_{12}, $Na_{0.23}TiO_2$, SnO_2, Co_3O_4, $NiCo_2O_4$, Sb_2O_3, Fe_3O_4, and Cu_2O are a few of the metal oxides known to mix with MXenes to create composites. The one with the highest reversible capacity (1330 mAh/g at 0.1C with 100Cycyles at 1C) is a spray-coated $Ti_3C_2T_x$-$NiCo_2O_4$ hybrid film electrode [38].

Zhao et al., manufacture $Ti_3C_2T_x$-CNT composites for capacitors. When CNT and $Ti_3C_2T_x$ layers are successively placed on top of one another $Ti_3C_2T_x$-CNT composite arises from the layered arrangement resembling a sandwich. Volumetric capacitance of the $Ti_3C_2T_x$-CNT electrode experiences an increase from 340 to 370 F-cm-3, marking an approximately 55% enhancement compared to the $Ti_3C_2T_x$ electrode after 10000 cycles that show growth of roughly 55% retention electrode after 10000 cycles [39].

Extraordinarily high discharge capacity of $LiNi_{0.8}Co_{0.1}Mn_{0.1}O_2$ (NCM811) >200 mAh/g is drawing more and more attention. However, its large-scale practical applicability is

constrained by insufficient mechanical strength, cycle stability, and rate capability. Yi Liao et al., 2021 show that MXene ($Ti_3C_2T_x$), a few-layer and rod-like addition, considerably improves the Li/NCM811 cells' mechanical characteristics, cycle efficiency, and rate capacity. The NCM811 contains 2.5 weight percent MXene (2.5-MXene) also offers greatest rate performance with a high discharge capacity of 209 Ah/kg at 0.2 C as well as high reversible capacity of 95 mAh/g at 8 C. In comparison to the pure NCM811 without MXene, capacity retention of 2.5-MXene may achieve 77.0% after 100 cycles at 0.5 C rate. Superior performances are the result of the efficient and multipurpose. The incorporation of MXene additive contributes to the enhancement of a more effective conductive network, facilitates the storage and release of Li+ ions through cation intercalation, provides increased room for deformation, forms a protective physical interface layer at the cathode-electrolyte interface, and mitigates the M→H2 phase transition within NCM811 electrodes [63].

Surface terminations on MXene greatly affect their mechanical properties. It is expected that MXenes ended by other groups (F and OH) would have lower stiffness than MXenes terminated by O. Compared to F or OH terminated MXenes, O-terminated MXenes often exhibit worse lattice properties. For example, Guo et al., found that functionalizing Ti_2C will decrease its young's modulus, yet functionalized Ti_2C can sustain more strain than uncovered Ti_2C and even graphene. The chemical formula of MXene, $M_{n+1}X_n$, which yields n as the number of atomic layers, also affects the mechanical characteristics of MXene. In their study, Yorulmaz et al. explore the Young's moduli and elastic constants of unmodified MXenes through classical molecular dynamics. Among various Tin+1Cn (n = 1, 2, and 3) compositions, the thinnest Ti2C material exhibits the highest Young's modulus, with its elastic constant approximately double that of MoS_2 [64]. According to Borysiuk et al., the strength and hardness of $M_{n+1}X_n$ T_x steadily increase when n is decreased. A composite made of polymers or carbon nanotubes is discovered to improve the mechanical characteristics of MXenes in experiments. $Ti_3C_2T_x$-polyvinyl alcohol composite exhibits high tensile and compressive strength while still being very flexible. $Ti_3C_2T_x$ -PVA composites have tensile strengths that are about four times higher than isolated $Ti_3C_2T_x$ [62].

Electrochemical properties

Because of their wide range of compositional possibilities, many surface functionalization options, and adaptable thickness controllability, MXenes may exhibit a wide range of electrical characteristics, from metallicity and semi-conductivity to topological

insulative. From 1.8 eV to 8 eV, metallic MXenes may vary greatly. The WFs of MXenes are shown to be more sensitive to their surface chemistry than the naked surface for a particular MXene. The WFs of all OH-terminated MXenes are very low (2.8 eV), nearly as low as Sc, which is the lowest among elemental metals. While Pt has the largest WF among all elemental metals, certain O-terminated MXenes have WFs that are considerably greater. Notably, in recent investigations, The WFs of MXenes often revert to an intermediate value due to the mixing of F, O, and OH groups on the MXene surfaces [65]. $Ti_2C(OH)_xF_y$ computed work function by Xu et al., to be ~98 eV. Hence, precise management of the surface functional group types is essential to attain the ultralow (or ultrahigh) work function of OH (or O)-terminated MXenes [66].

It has been hypothesized that typical two-dimensional semiconductors like transition metal dichalcogenides and blue phosphorene have the potential to establish n-type Schottky barrier-free interfaces with OH-terminated MXenes featuring ultralow work functions. Six materials (V_2CO_2, Cr_2CO_2, Mo_2CO_2, $V_4C_3O_2$, Cr_2NO_2, and V_2NO_2) connections to MoS_2 with disappearing p-type schottky barriers at MoS_2-MXene interfaces. This enables very effective hole injections into MoS_2 [67].

Conductivity of MXenes may vary from less than 1 S/cm^1 to hundreds of S/cm^1, and this greatly relies on the processes used in their synthesis and delamination. For instance, HF-etched $Ti_3C_2T_x$ has a conductivity of just 2 S/cm^1, but LiF + HCl-etched $Ti_3C_2T_x$ has a conductivity that might reach 1500 S/cm^1. When $Ti_3C_2T_x$ that has been etched with LiF+HCl delaminates, its conductivity is increased even further. In practical applications, the combination of MXenes with other promising electrode materials is a common approach to create composites that demonstrate exceptional electrochemical properties in lithium-sulfur batteries and lithium-ion batteries. While SnO_2- $Ti_3C_2T_x$ is based on an alloying/dealloying mechanism and TiO_2-$Ti_3C_2T_x$ on an intercalation/deintercalation mechanism, Fe_3O_4-$Ti_3C_2T_x$ and Co_3O_4-$Ti_3C_2T_x$ both employ a special "conversion reaction" process. The exceptional electrochemical characteristics of $Ti_3C_2T_x$-TMO composites are best electrical properties [68].

Chapter No. 3

Materials and Methods

In the first section of this chapter, we have studied experiments conducted during the synthesis of the nanoparticles and the synthesis method used for the preparation of these nano materials. Synthesis of (NMC811-$Ti_3C_2T_x$) nanocomposite and its electrode fabrication is discussed after through a description of molten salt etching method for producing ($Ti_3C_2T_x$) and co-precipitation method and solid-state reaction method for producing $LiNi_{0.8}Mn_{0.1}Co_{0.1}O_2$ (NMC811) nanoparticles. In second part we described the experimental techniques used to characterize ($Ti_3C_2T_x$), (NMC811) and (NMC811-$Ti_3C_2T_x$) nanocomposite.

3.1 Materials

3.1.1 Required materials for synthesis of MXene

Chemicals

Chemicals	**Chemical formula**	**Molar mass**	**Purity**
MAX-Phase (312)	Ti_3AlC_2	134.73g/mol	>98.9%
Ammonium-per sulphate	$(NH_4)_2S_2O_8$	228.18 g/mol	99%
Potassium Chloride	KCl	74.55 g/mol	>98.9%
Sodium Chloride	NaCl	58.44 g/mol	>98.9%
Copper-Chloride (Anhydrous)	$CuCl_2$	134.45 g/mol	>98.9%

3.1.2 Required materials for synthesis of (NMC811)

Chemicals

Chemicals	**Chemical formula**	**Molar mass**	**Purity**
Ammonia-hydrated solution	$NH_3.H_2O$	35g/mol	26%
Cobalt-sulfate heptahydrate	$CoSO_4.7H_2O$	281.1g/ mol	99%
Lithium-hydroxide monohydrate	$LiOH.H_2O$	42g/mol	99%
Manganese-sulfate monohydrate	$MnSO_4.H_2O$	169 g/mol	99%
Nickle-sulfate hexahydrate	$NiSO_4.6H_2O$	262.7 g/mol	98%
Sodium hydroxide	NaOH	40 g/mol	98%

3.2 Synthesis and synthesis methods

3.2.1 Molten salts etching method

The majority of synthesis techniques are ineffective for etching MAX-phase precursors with A-site elements other than aluminum, such as Si, Ga, and Zn, displaying them unsuitable for such precursors. The range of potential MAX-phase precursors was expanded in 2020 proposed is a Lewis molten salt etching technique designed for the selective etching of MAX phases, incorporating different A-site elements. MXenes, however, are chemically unstable due of their oxidation sensitivity, especially at high temperatures.

In 2019, a molten salt (MS^3) process was innovated for generating oxidation-sensitive materials in air atmosphere environment like porous Ti, Ti_3SiC_2, and Ti_2AlN MAX-phases. In this method, a low-melting-point KBr acts as a reaction medium, protecting products against oxidation throughout high-temperature synthesis. This is achieved by creating a protective shield of molten salt around the sample, even at lower temperatures. We have recently proposed an innovative technique to fabricate MXenes, which employs a one-pot molten salt synthesis approach. In this method, we utilize M, A, and X (carbon) elements as the precursors for the

successful fabrication process, molten salt technique used in the synthesis of MAX-phases and the Lewis-salt etching method for creating MXenes. Identical MAX- phases have been utilized as precursors in molten salt process utilized for MXene production involved the utilization of $CuCl_2$ lewis salt as the etchant. In a similar manner, a molten salt environment was created using low-melting-point eutectic chlorides (NaCl + KCl) as the salt bed. Purpose of molten salt is preventing direct contact between high temperature air and the reactants. Without inert gas shielding, some carbide MXenes and nitride MXenes that are generally challenging to obtain by normal methods were effectively synthesized in a much less time [25].

Figure 3.2.1 Molten salt-shielded synthesis process for producing ($Ti_3C_2T_x$) MXene in an air atmosphere [25].

Synthesis of MXene

The first step involved combining molten salt (NaCl: KCl = 1:1 stoichiometric molar ratio) with 0.5g of Ti_3AlC_2 MAX-phase powder in a weight ratio of 1:4-6. The mixture was grinded using a mortar and pestle for a duration of 20 minutes. The resulting powder was then uniformly pressed in a hydraulic presser to form a pellet. (To keep MAX-phase from potentially oxidizing during the heating process, the NaCl/KCl-pressed MAX-phase precursors are put together into a pellet. The cylindrical-shaped final pellet was placed into a crucible. Subsequently, it underwent grinding for 10 minutes. A separate crucible, also with a capacity of 30 mL, was filled with a salt solution containing 8.766g of NaCl, 11.183g of KCl, and 2.073g of $CuCl_2$. This prepared solution was then added to cover the pellet. The pellet was introduced into a furnace, which was heated to 700°C at a rate of 10°C per minute. The temperature was then maintained at 700°C for a duration of 10 to 40 minutes. with a lid on top. The $Ti_3C_2T_x$/Cu combination was repeatedly washed with deionized-water to eliminate out ions after reaching RT. Washing the resulting ($Ti_3C_2T_x$/Cu) mixture for 1 hour at room temperature with 100 mL

of 0.5M APS solution removed the Cu from mixture. After multiple washing with deionized water, the resulting solution was filtered. Subsequently, the ($Ti_3C_2T_x$/Cu) MXene powder was subjected to a vacuum drying process at room temperature for a duration of 12 hours [36].

Preparation steps

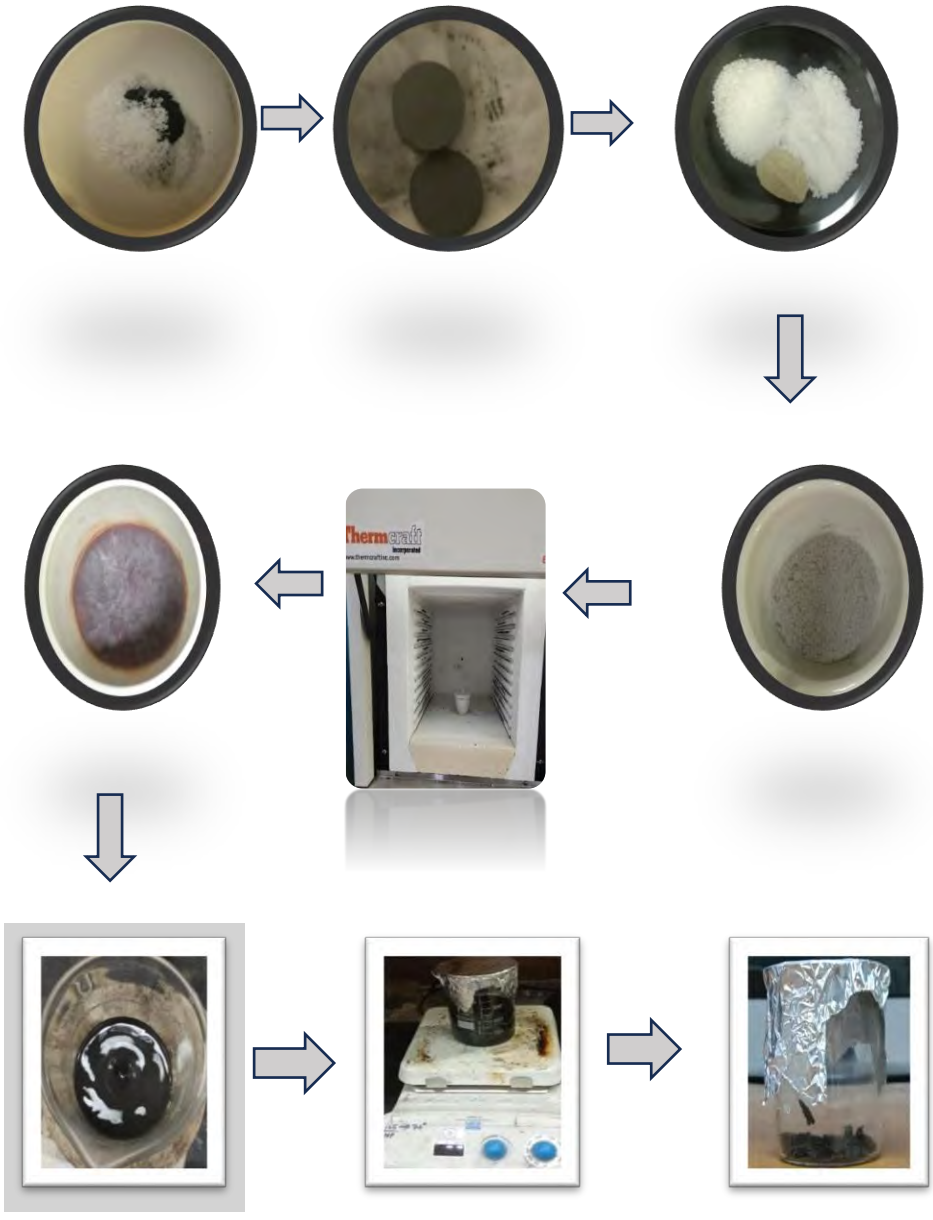

3.2.2 Co-precipitation method

Importance of the co-precipitation technology is increasing for spreading the precursors and components used in a reaction to produce the necessary sample. Co-precipitation approach is used to create materials with dual functions by creating comparable precipitates that closely

mix elements during precipitation while keeping chemical homogeneity throughout calcination. In the co-precipitation method, transition metal salts are mixed with a base that acts as a precipitating agent at ideal temperatures. However, this synthesis technique is frequently used [69]. Co-precipitation approach has the benefit of producing crystalline sizes, the co-precipitation method exhibits a significantly narrower range of variation compared to other synthesis processes. Co-precipitation technique has significant drawbacks, this method involves continuous washing, drying, and calcination steps to achieve the production of a pure phase. Co-precipitation approach has advantage that the precursors behave uniformly at the molecular level. Co-precipitation method has many benefits, such as a high number of finished products, transparency and purity, simplicity of responsibility, and low cost [70].

3.2.3 Solid-state reaction method

Solid state reaction technique used frequently to synthesize polycrystalline materials from solid reagent. In this method synthesizing a compound by mixing solid precursors and heating them a high temperature in reactive environment. Effectiveness and large-scale production are two advantages of the solid-state reaction approach. Temperature required for solid to react is 1000°C-1500°C. The success of the solid-state reaction relies on multiple factors, including reaction conditions, structural attributes of the reactants, solid's surface area, and their inherent reactivity. It is cost defective, minimum waste of material, but it is challenging for getting high purity of material and homogeneity in final product [71].

Synthesis of lithium nickel manganese cobalt oxide

For preparation of nickel, manganese and cobalt stoichiometric solution with ratio 8:1:1 respectively, take 21g $NiSO_4.6H_2O$ with 40 ml of deionized-water, 1.69g $MnSO_4.H_2O$ with 5ml of deionized-water and 2.81g $CoSO_4.7H_2O$ with 5ml of DI-water in a three separate beaker. All three-solution stirred for 2-hours. After that three well stirred solution mix in a beaker and again stirred for 2-hours at 50°C. 2M $NH_3.H_2O$ solution and 4M NaOH solution added dropwise in a mixture of transition metals stirred solution of 50°C. Upon adding $NH_3.H_2O$ solution and NaOH solution in transition metals solution, solution changes PH. When PH maintain 11.5-12.0, then stop adding $NH_3.H_2O$ and NaOH solution and put on stirrer for 24-hours at 50°C temperature again for proper mixing of three solution. After 24-hours precipitates are collected, centrifuged (washed with 500milli litre deionized water), precursors separated and put in dryer at 90°C for a night.

Dried precursors collected and weighted, add $LiOH.H_2O$ with 5% excess of total weight of dry precursor, then both grinded well with the help of mor-tor pestle. Make pellets of grinded mixture and put in tube furnace for 12-hours (place in boat crucible) in the presence of oxygen flow at 800°C temperature. After 24 hours boat crucible gets out from tube furnace carefully and grinded pellets well for obtain $LNMCO_2$ (NMC811) powder [27].

Preparation steps

3.2.4 Coating of different materials on (NMC811) cathode material

Enhancing the performance and stability of (NMC811) cathode materials can be achieved through the application of various coating materials. These coatings serve multiple purposes, including improving electrode-electrolyte interface, mitigating undesirable side reactions and enhancing the structural stability of the cathode. NMC811 stands out as a high-voltage cathode material for lithium-ion batteries. It boasts an impressive specific capacity of 200 mAh/g and is characterized by an upper cut-off voltage of 4.3 V vs Li/Li+. Unfortunately, Typically NMC-based lithium-ion batteries have been associated with low cycling stability, this phenomenon can be ascribed to the oxidation of the electrolyte at the cathode surface, along with structural alterations in the materials occurring at high potentials or temperatures. The purpose of surface coating is to enhance coulombic efficiency and cycling stability, it is possible by removing lithium compounds and prevention from parasitic reaction. Zhang et al., proposed a simple coating procedure that involved ball milling a suspension of N-methyl pyrrolidinone (NMP) NMC-$LiPF_6$ and $LiPF_6$ as a cathode additive. The Li/NMC811 cells' cycle stability and rate capability were both increased by coating of Li_3PO_4-LiF on NMC surface as a result of the milling procedure. Stable LiF dominates the coated surface of Li_3PO_4-LiF as a result of stable solid electrolyte Li_3PO_4-LiF [41].

Li/NCM811 cells' mechanical properties, cycle performance, and rate capability are all greatly improved by rod-like MXene ($Ti_2C_3T_x$), a multifunctional addition. It helps in creating a more effective conductive network, cation intercalation storage and release of Li+, by offering additional deformation space, creating a physical protective solid electrolyte interphase layer, and suppressing the M→H2 phase transformation, NCM811 electrodes can be effectively improved [63]. The cathode powder of $LiNi_{0.8}Co_{0.1}Mn_{0.1}O_2$ (NMC811) was coated with Li-Nb-O through a wet chemical method, utilizing lithium niobium ethoxide as the precursor giving the material a coating/substitution co-modification that greatly enhances electrochemical performance [72]. NMC811 cathode materials are frequently coated with carbon-based materials to improve their electrical conductivity, such as carbon nanotubes or carbon black. The incorporation of carbon coatings can enhance the overall battery performance, including rate capability and cycling stability [73].

NMC811 cathode coated with metal oxides like (Al_2O_3), (TiO_2), or (SiO_2) to increase structural stability and lessen undesirable side reactions. Researchers have looked into polymer coatings like polyvinylidene fluoride (PVDF) or polyethylene oxide (PEO) to increase the

stability and cycling performance of NMC811 cathodes. Cathode structure mechanically supported by polymer coatings, which improve the presence of carbon coatings enhances the adhesion between cathode particles, thereby reducing their dissolution of transition metals into the electrolyte. Composite coatings mix many materials to benefit from each one's unique properties. For example, the simultaneous improvement of electrical conductivity and structural stability has been explored for a carbon-coated NMC811 cathode with an extra metal oxide coating [73].

It's crucial to remember that the selection of the coating material is influenced by a number of variables, including the particular battery application, economic concerns, and production methods. Improve functionality and durability of NMC811 cathode materials, researchers are still investigating various coating techniques.

3.2.5 MXene coating on (NMC811)

First of all, ~0.003g of MXene and 0.085g of NMC811 (2.5 wt.% of MXene with respect to NMC811) individually sonicate 2 hour with ethanol for proper dispersion. Then both collected in beaker and put for drier at 80°C for 6 h. After that coated (MXene on NMC811) material obtained. Similarly, procedure repeated for 4% and 10% composite of MXene with NMC811 (MXene (0.032g) and NMC811 (0.8g) and (MXene (0.06g) and NMC811 (0.6g) respectively [39].

3.2.6 Electrode fabrication of Pristine NMC811/$Ti_3C_2T_x$-NMC811

For the manufacture of electrodes, a weight ratio of 80%, 10%, and 10%, respectively, of the active material NMC811, Acetylene-carbon black, and polyvinylidene-difluoride (PVDF) is used. 0.01g of PVDF dissolved in 0.25mL of NMP solvent in glass bottle and stirred for 4-5 hours. Then 0.08g of active material (NMC811) and 0.01g of carbon black added above stirred solution and put on stirring for overnight for making gluey slurry. The slurry was subsequently brushed on nickel foam and allowed to dry for 12 hours at 80°C in a drying oven. The same procedure is done for the $Ti_3C_2T_x$ -NMC811(2.5 wt%) composite, which contains 0.08g of the active ingredient and $Ti_3C_2T_x$ as an additive (coated) on pristine NMC811. In case of $Ti_3C_2T_x$-NMC811(2.5 wt%) composite, weight of nickel foam cathode is 0.11g, in which material loading weight is 0.063g. while for pristine NMC811 cathode, weight of nickel foam cathode is 0.05g, in which material loading weight was 0.025g, and $Ti_3C_2T_x$ as an additive

(coated) on pristine NMC811 weight of nickel foam cathode is 0.06g in which material loading weight was 0.03g.

3.3 Characterization Techniques

This portion will contain brief introduction of characterization techniques for nanomaterials, that are used to characterize our materials.

3.3.1 X-ray Diffraction

X-ray diffraction (XRD) is a technique employed to analyze the atomic and molecular structure of materials, utilizing the principles of X-ray diffraction theory. X-ray diffraction technique, which was initially presented by Max von Laue in 1912, was further developed by William Henry Bragg and his son William Lawrence Bragg. The basic principle is that when x-rays target on a crystalline substance, the x-rays interact with the atoms in the crystal lattice and are diffracted, or dispersed, in a pattern. The atom arrangement within the crystal is shown by this diffraction pattern. Depending on their variation in course, the scattered x-rays can interfere either positively or negatively. It is mathematically described as $n\lambda=2d\sin\theta$, in Bragg's Law, "n" represents the order of diffraction, "λ" denotes the wavelength of x-rays, "d" signifies the distance between neighboring lattice planes in the crystal, and "θ" represents the angle at which the x-rays are incident.

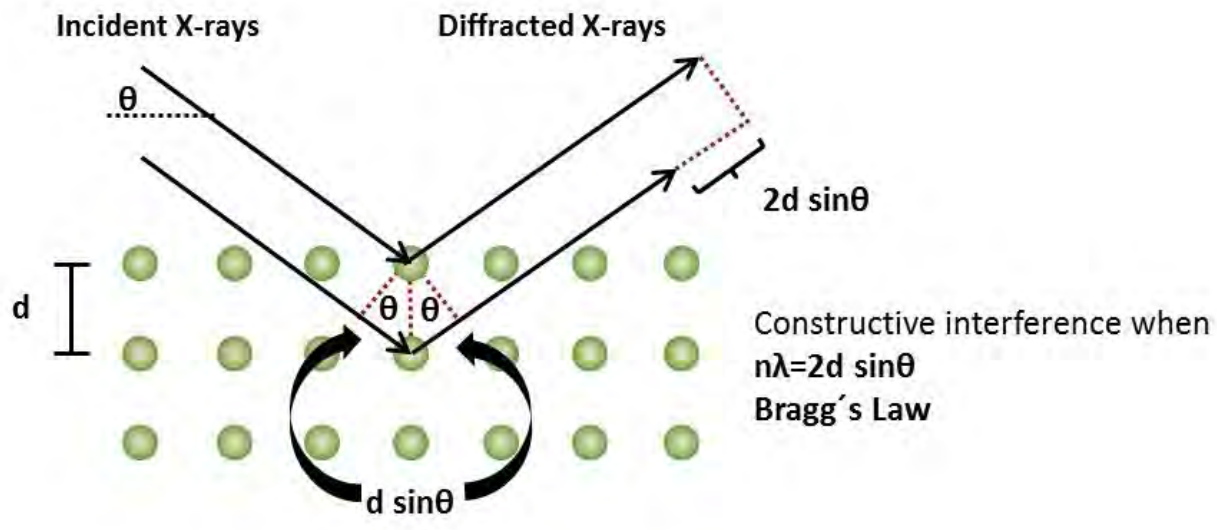

Figure 3.3.1 XRD Mechanism [https://wiki.anton-paar.com]

A sample is exposed to a monochromatic (single wavelength) x-ray beam, angles and intensities are measured when x-rays are diffracted by the crystal lattice. A detector, whether it

be photographic film or a digital detector, captures the diffracted x-rays, and subsequently, the resulting diffraction pattern is recorded. The constructive interference of x-rays dispersed by various atom planes inside the crystal lattice results in a succession of brilliant spots or peaks that are seen in the diffraction pattern at particular angles. Different structural characteristics of the material, such as the distance between lattice planes, the crystal structure, the orientation of crystal domains, and the existence of any impurities or defects, can be identified using these angles and intensities.

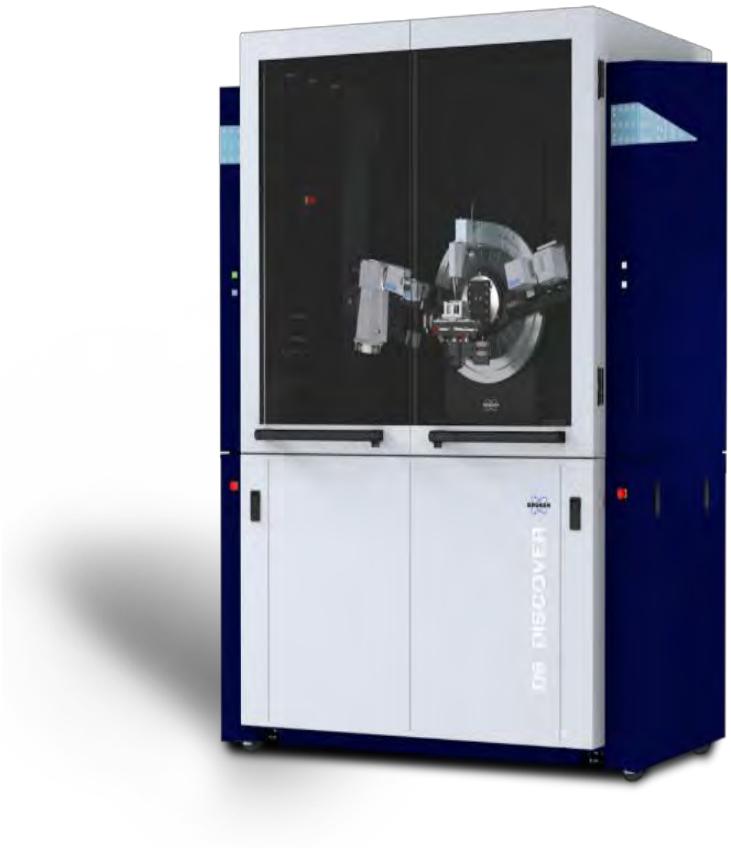

Figure 3.3.2 XRD Machine [https://www.bruker.com]

Based on x-ray diffraction data, Scherrer's formula, commonly referred to as the Scherrer equation, is a mathematical formula used to find the typical size of crystalline particles in a solid substance. In 1918, swiss scientist Paul Scherrer created it.

The formula is written as follows:

$$\mathbf{D = K\lambda / (\beta \cos \theta)}$$

Where:

D is the average crystallite size

K is the Scherrer constant, which depends on the shape of the crystalline particles (usually taken as around 0.9)

λ is the wavelength of the X-ray radiation used

β represents the full width at half maximum (FWHM) of a diffraction peak, which serves as a measure of the peak broadening.

θ is the Bragg angle, the angle of incidence of the X-rays on the crystal surface

According to Scherrer equation, the material's crystalline particles, which are finite in size, are the only factor contributing to the peak broadening. It takes into account how these particles affect x-ray diffraction and links to observed broadening of diffraction peaks to particle size.

3.3.2 Scanning Electron Microscope and Energy Dispersive X-ray Spectroscopy

It is advance tool for study of structural details of nanomaterials. SEM technique use electrons for imaging of materials. We can investigation the metallographic details, imperfections, topology and morphology, such as particle sizes and shapes of nanocrystalline powders and bulk materials.

SEM instrument includes these components:

- Electron source
- Anode
- Condenser lens
- Scanning coils
- Objective lens

Electrons are produced by uppermost section of the microscope's column. These electrons are drawn by the positive charge on the anode plate, thus creating a beam of electrons. Number of electrons within the beam and its dimensions are controlled through the use of the condenser lens. The image resolution is contingent on the beam size, and apertures can also be employed to regulate the beam's size. The beam moves in a rectangular path across the sample's surface, the scanning coils are utilized for deflecting the beam along both the x and y axes. The objective

lens, which is the last lens in the series, plays a crucial role in producing the electron beam. It focuses the beam to a tiny point on the sample, given its position as the lens closest to the sample. SEM lenses are electromagnetic and composed of a coil of wires. Due to magnetic field current flow through these coils and electrons allows the microscope's lenses to exert precise control over them.

This technique is helpful collecting information like image of materials, morphological studies of materials like sample is hollow or solid, sphere or square, pores or non-pores etc. Normally use micro-size (10^{-6}) and nano-size (10^{-9}) for image and high resolution. We can measure diameter/ area of materials at micro and nano scale level.

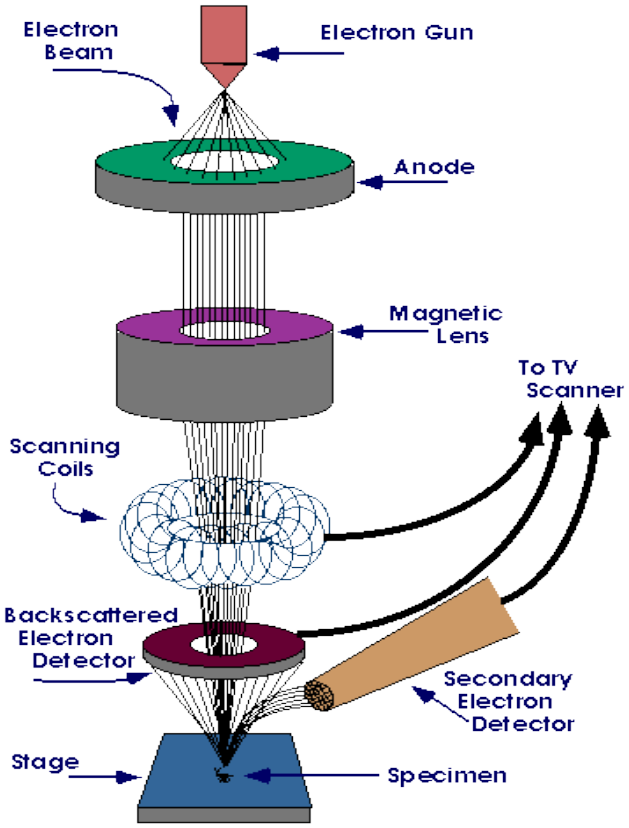

Figure 3.3.3 SEM setup [http://emicroscope.blogspot.com]

Energy-dispersive X-ray spectroscopy (EDS) is a analytical method utilized for conducting elemental analysis and chemical characterization of materials. It is also known as energy dispersive x-ray analysis or energy dispersive x-ray microanalysis. EDS relies on the interaction between an x-ray excitation source and a sample. It is built in SEM setup.

3.3.3 Cyclic voltammetry

Cyclic voltammetry (CV), an electrochemical technique, is employed to examine the redox properties of a chemical species. It includes giving an electrochemical cell a controlled potential waveform and measuring the resulting current. Cyclic voltammetry functions by applying a potential waveform to an electrochemical cell and then observing and measuring the resulting current.

An electrochemical cell with a working electrode, a reference electrode, and a counter electrode makes up a common CV-configuration. The working electrode is typically constructed from a substance that interacts with the desired electroactive species. In the context of current flow, the counter electrode serves to complete the circuit, whereas the reference electrode provides a stable potential reference. By sweeping the potential repeatedly between two predetermined limits, a potential waveform is applied to the working electrode. Although alternative waveforms and scan rates can also be employed, the potential is normally swept linearly at a fixed scan rate. Between the electrode and the species, there is an electron transfer during these reactions. An ammeter is used to measure the resultant current that flows through the electrochemical cell. Voltammogram is a useful tool for learning about a system's electrochemical behaviour. Peak potentials and placements provide information about the oxidation.

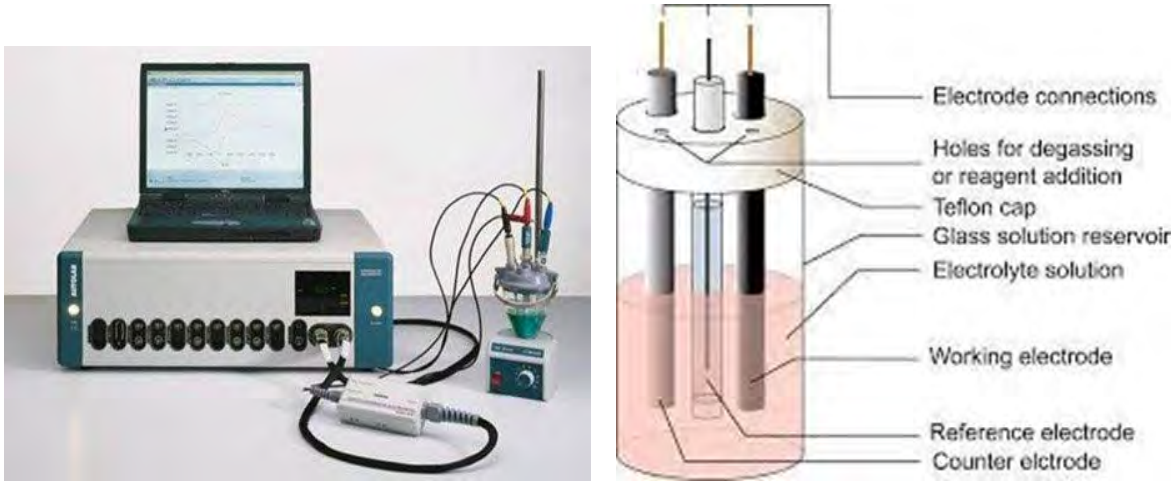

Figure 3.3.4 Cyclic Voltammetry setup [https://pubs.acs.org/doi/10.1021/acs.]

Chapter No. 4

Results and Discussions

In this chapter we have discussed result and testing of prepared nano-materials NMC811, $Ti_3C_2T_x$ and nano-composite (NMC811-$Ti_3C_2T_x$). (NMC811) nanoparticles synthesized by co-precipitation and solid-state reaction method, while MXene ($Ti_3C_2T_x$) was prepared by molten salt etching method. After that MXene coated cathode prepared by using wet-chemical method ethanol as a solvent. We used XRD, SEM, EDX and CV characterization for investigation of our prepared materials.

4.1 X-ray Diffraction

Nano particles of $LiNi_{0.8}Co_{0.1}Mn_{0.1}O_2$ prepared by co-precipitation and solid-state reaction method, and $LiNi_{0.8}Co_{0.1}Mn_{0.1}(OH)_2$ precursor prepared by co-precipitation method. X-ray diffraction (XRD) results are measured by using Cu K-α radiation (λ=1.54nm with range of 2θ =10 ° to 80°). We have observed all characteristics peaks of $LiNi_{0.8}Co_{0.1}Mn_{0.1}O_2$ are well matched with pure $LiNi_{0.8}Co_{0.1}Mn_{0.1}O_2$ (NMC811) literature review data and peaks appeared at the same angle which show well crystalline structure. Peaks angle and miller indices (hkl) values are matched from its (JCPDS) card (96-152-0790). Peaks indices are (003), (101), (006), (104), (015), (107), (108), (113), (021) show hexagonal and well crystalline material. The I_{104}/I_{003} ratio is 1.44 at 800°C indicate that lower order of cation (Ni^+/Li^+) mixing in this material. According to the XRD patterns, pristine NMC811 is a single-phase multi-layered-rhombohedral ($LNMCO_2$) with R-3m space group.

XRD pattern of $LiNi_{0.8}Co_{0.1}Mn_{0.1}(OH)_2$ show P-3m space group, all diffraction lines are indexed to hexagonal structure and all peaks appeared at the same angle and well matched with literature data. The I_{111}/I_{100} ratio is 1.50 exhibit lower order of cation (Ni^+/Li^+) mixing. After that we coat pristine NMC811 with MXene by using ethanol as a solvent. XRD results (figure 4.2) show that all peak intensity becomes reduced by coating, looking crystalline all these peaks are indefinable with that $LiNi_{0.8}Co_{0.1}Mn_{0.1}O_2$. The average crystallite size of the pure NMC811 and $Ti_3C_2T_x$ -NMC811 was determined by Scherrer formula is 50nm and 33nm respectively.

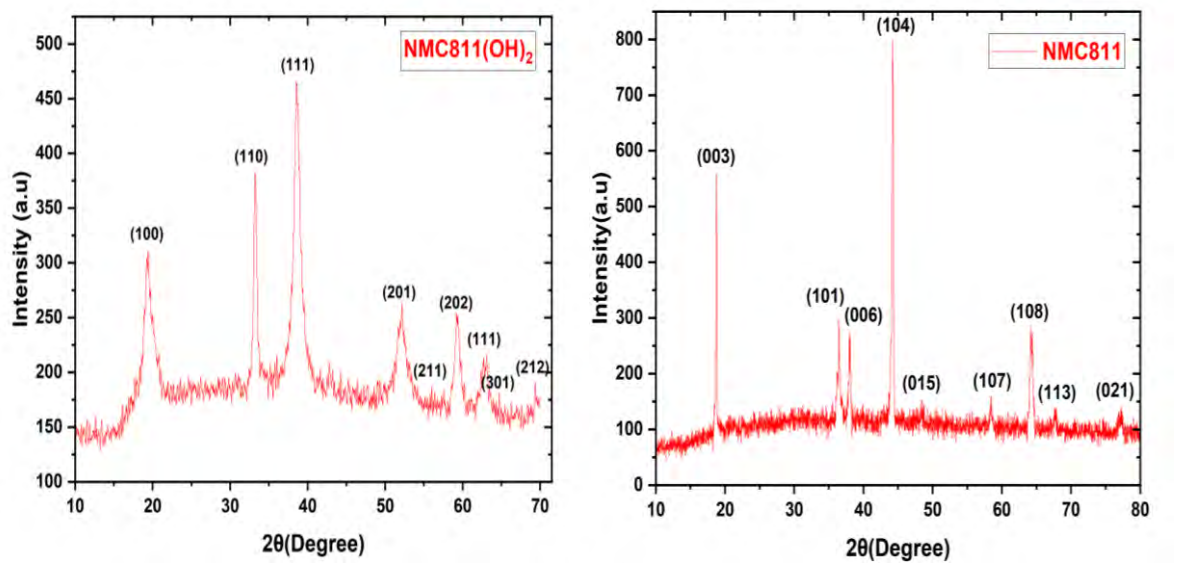

Figure 4.1 XRD pattern of $NMC811(OH)_2$ precursor and pristine NMC811

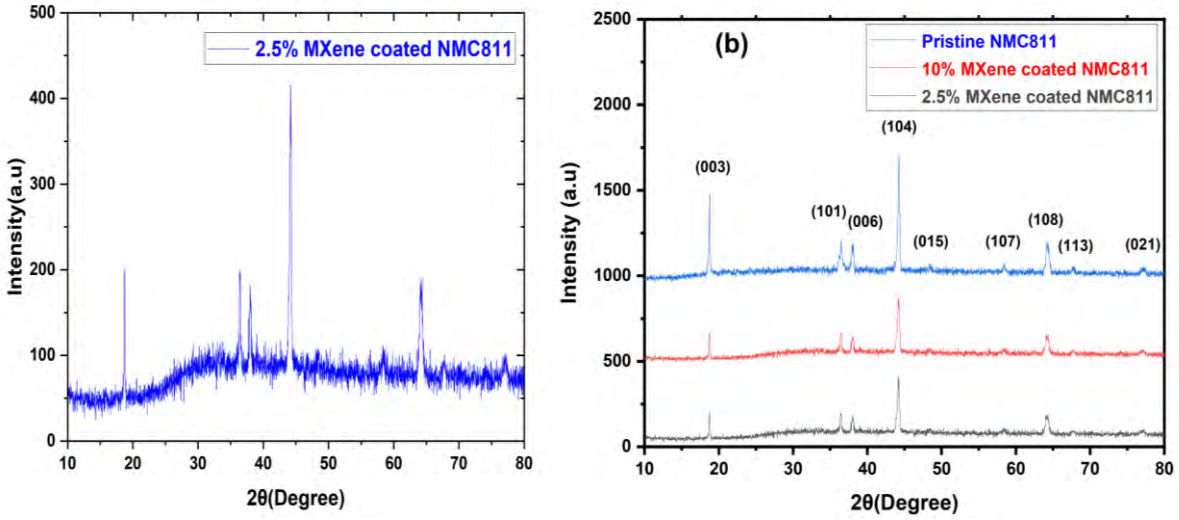

Figure 4.2 XRD pattern of 2.5% wt. of MXene coated NMC811 and stacked graph of pure NMC811, 10% and 2.5% wt. of MXene coated NMC811

Figure 4.3 show XRD pattern of Ti_3AlC_2 precursor and stacked graph with MXene ($Ti_3C_2T_x$) before and after molten salt etching for 10-40min at 700°C with 1 hour and 10 mins ramp time and 40 mins soaking time. After 40 mins of etching, the diffraction peaks of Ti_3AlC_2 (MAX-Phase) almost disappeared, while sharp diffraction peaks of the $Ti_3C_2T_x$ (MXene) were observed. After etching, the (002) peaks of the Ti_3AlC_2 shifted left from $2\theta=9.56°$ to $2\theta=9.30°$ with increasing interlayer spacing d=9.24nm from d=9.49nm which corresponds etching of aluminum from precursor. (004) peaks shifted from $2\theta =19.21°$ to $2\theta =18.98°$ with minimum intensity indicates almost aluminum removed from our materials. (008) peaks less intensity in

$Ti_3C_2T_x$ due to aluminum layer remove and surface functional group (T_x) introduce and one peak is disappeared due to etchant (Cu^{2+}) removed.

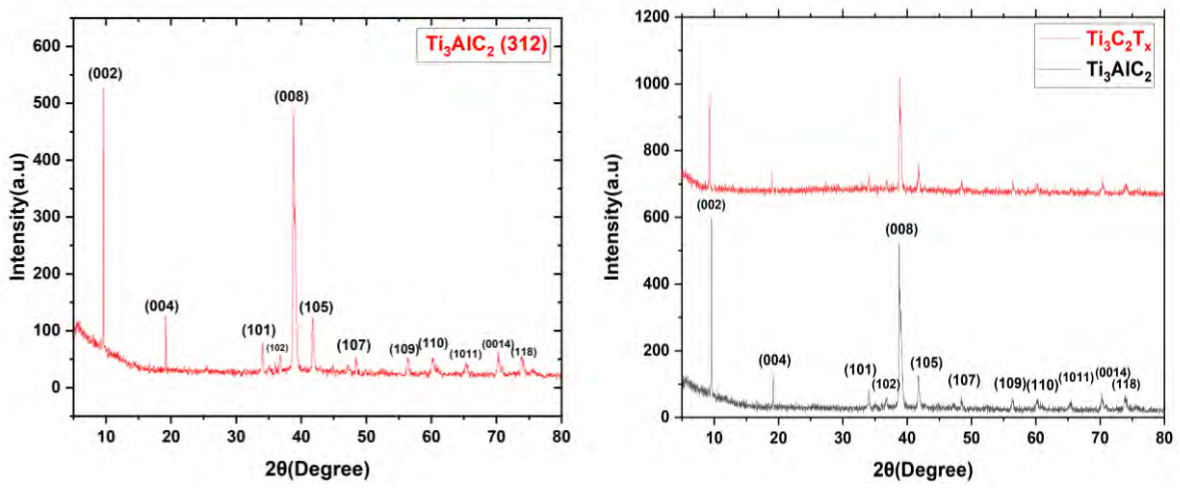

Figure 4.3 XRD pattern of Ti_3AlC_2 (312) precursor and stacked graph of Ti_3AlC_2 with ($Ti_3C_2T_x$)

4.2 Scanning Electron Microscope and Energy Dispersive X-ray Spectroscopy

Scanning electron microscopy (SEM) was used to study the particles shape and size (morphology) and distribution of $LiNi_{0.8}Co_{0.1}Mn_{0.1}O_2$ (pure NMC811) and $LiNi_{0.8}Co_{0.1}Mn_{0.1}(OH)_2$ precursor as shown in (fig 4.4) and (fig 4.5) majority of the particles seemed to have a spherical, cubic and rectangular shape (few particles) similar to a building block obtained and average particles diameter almost 150nm for pure (NMC811) and 5000nm for $LiNi_{0.8}Co_{0.1}Mn_{0.1}(OH)_2$ precursor. Change in particle morphology due to stirring rate of rpm during synthesis. EDS /EDX in SEM mode was used to create compositional maps. The chemical nature of the particles deduced using energy dispersive X-ray spectroscopy. The EDS maps spectrum of pristine NMC811 (fig 4.4) show Ni, Mn and Co elements have a uniform distribution over the particles. Atomic ratio of Ni: Mn: Co in the sample is measured to be 60%: 7%: 5%, which is approximately close to desired composition. The EDS maps spectrum of $NMC811(OH)_2$ precursor (fig 4.5) show maximum percentage of nickel with other elements (Mn, Co, O, S, and C). After adding $LiOH.H_2O$ salt in $NMC811(OH)_2$ precursor and sintering at 800°C for 12 h for obtaining NMC811 with desired ratio.

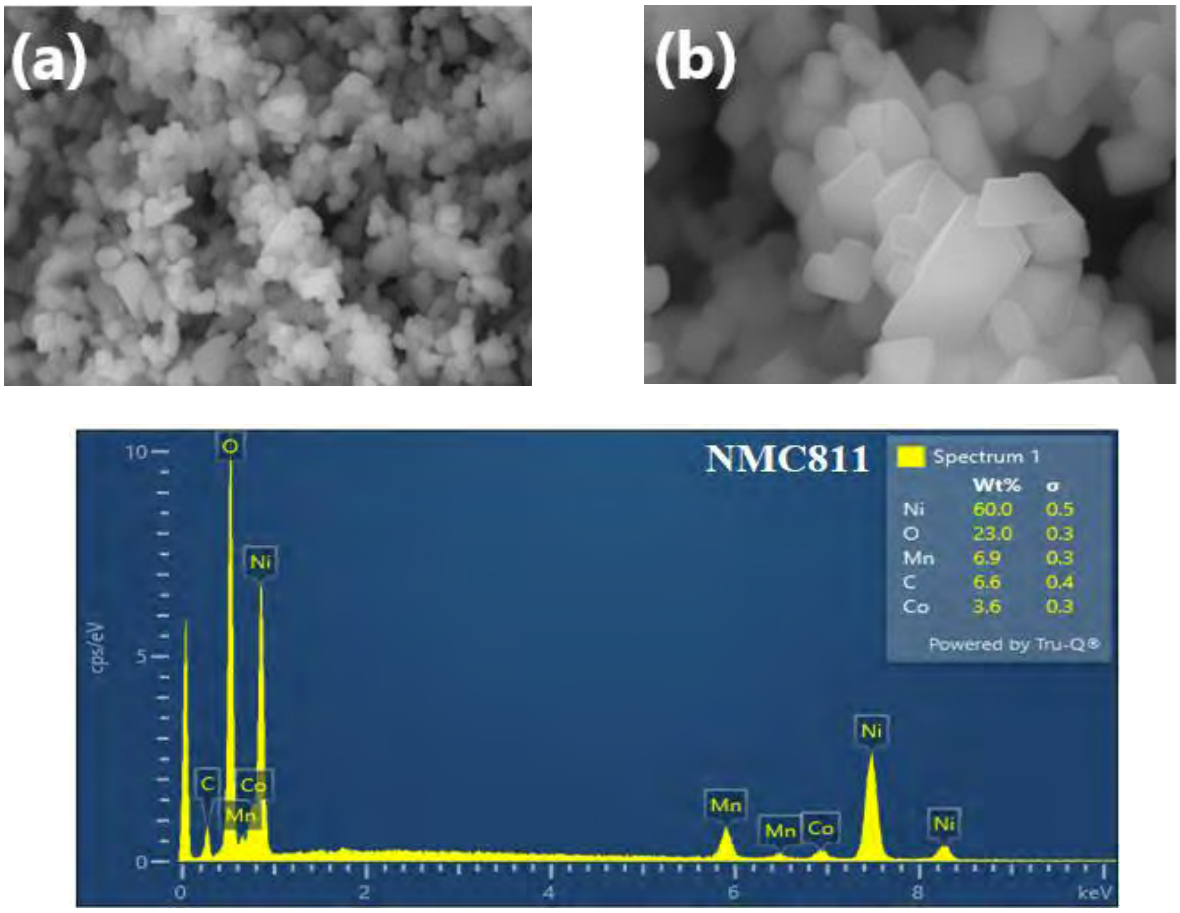

Figure 4.4 SEM and EDS spectrum of pristine NMC811

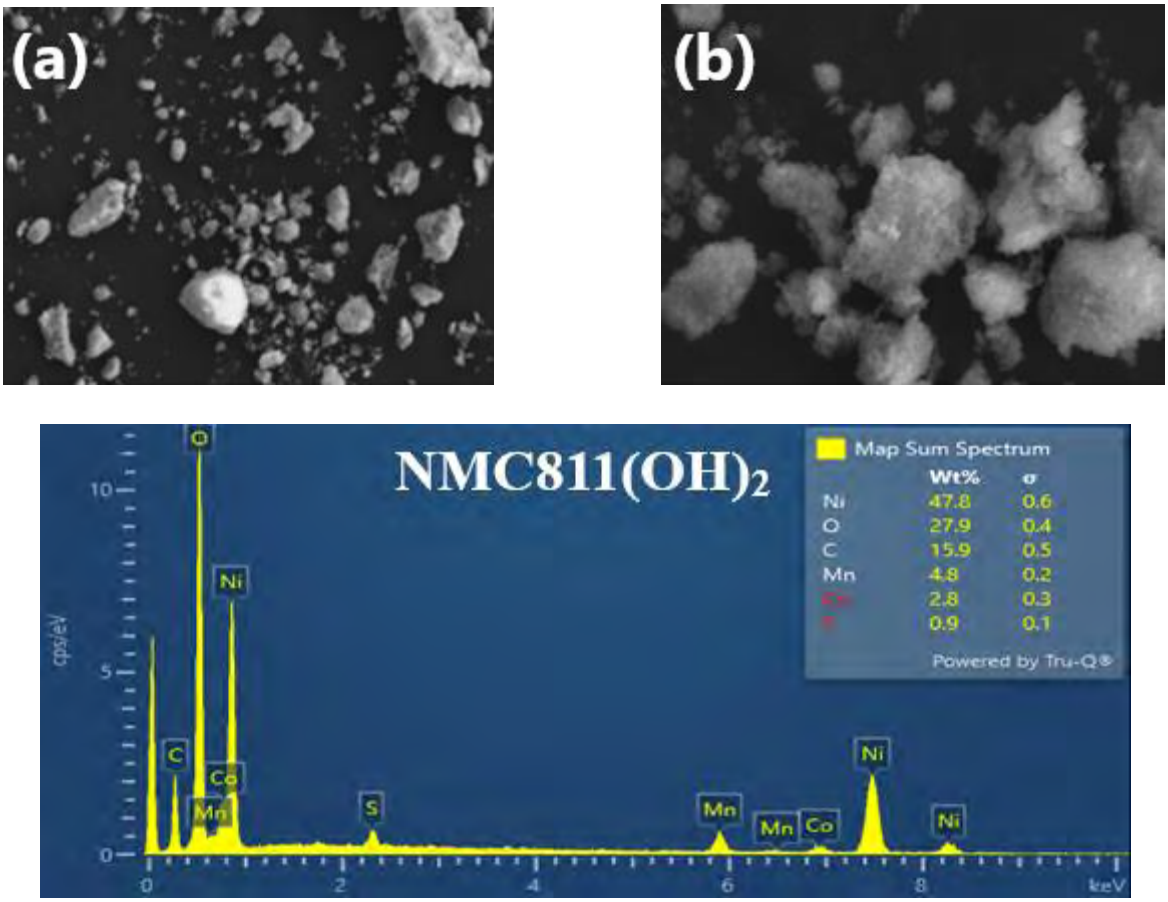

Figure 4.5 SEM and EDS spectrum of pristine $NMC811(OH)_2$ precursor

Figure 4.6 present scanning electron microscopy images of pristine Ti_3AlC_2 precursor layer ternary structure, in which A-layer in between transition metal carbide. Energy Dispersive X-ray spectroscopy (EDS) mapping of pristine Ti_3AlC_2 precursor show approximately 100% composition of Ti, Al and C elements. This ratio makes MAX-phase precursor for MXene (by removing Al almost Ti-Al ratio should be 3:0.02).

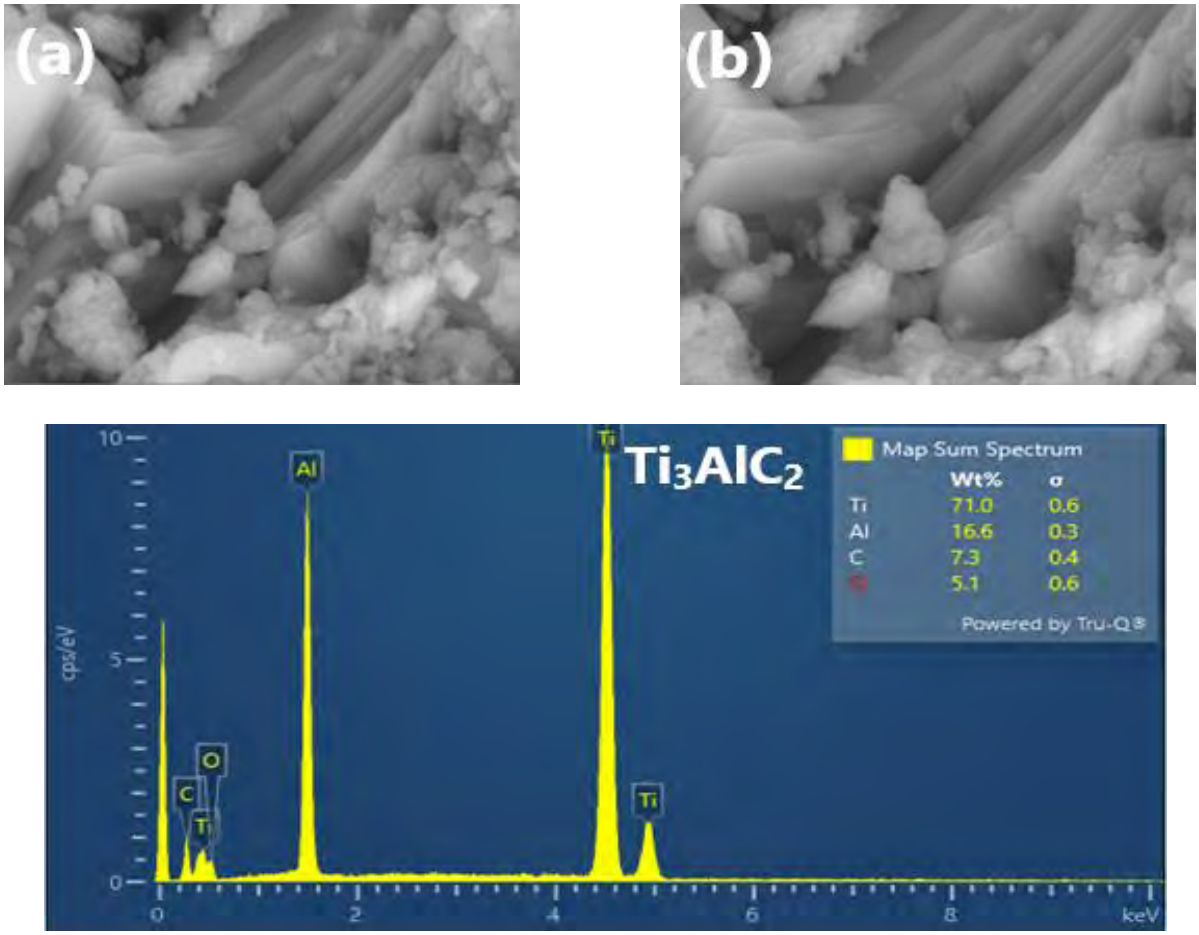

Figure 4.6 SEM and EDS spectrum of pristine Ti_3AlC_2 (312) precursor

Figure 4.7 displays scanning electron microscopy (SEM) images of $Ti_3C_2T_x$ (T_x=Cl) MXene, illustrate the characteristic and anticipated multilayered structure exhibited by all MXene particles. The images illustrate the separation of MXene sheets, with 60% aluminum being etched from the MAX-phase. Energy Dispersive X-ray Spectroscopy (EDS) mapping further indicate the presence and distribution of Ti, C, Al, Cl, Cu, and O elements. After 40 minutes of etching, the Al to Ti ratio significantly decreased from 1:3 to approximately 0.4:2.7, indicating the near-complete removal of Al from the original Ti_3AlC_2 precursor. Maximum composition of titanium is obtained as desired, Cl (surface group) and etchant Cu^{2+} (Lewis's acid) almost etched and obtained in 0.1 and 0.3 ratio respectively.

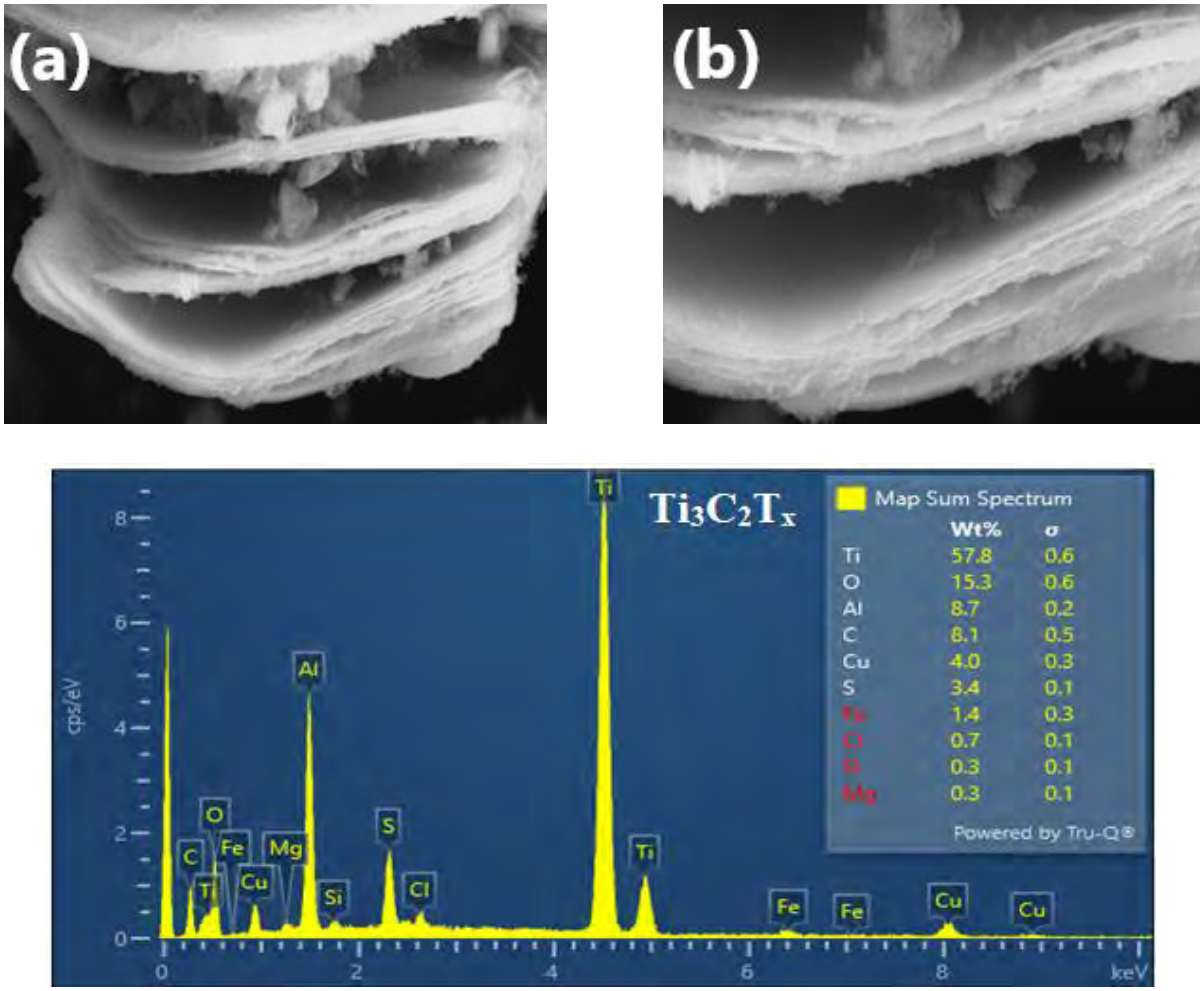

Figure 4.7 SEM and EDS spectrum of $Ti_3C_2T_x$ (MXene)

SEM images of MXene coated (NCM811) shown in (figure 4.8). The coating of MXene results in the creation of point-face and line contacts between transition metals that's increase empty spaces. This phenomenon contributes to the formation of an improved conductive network or channel, facilitating enhanced electronic and ionic exchange capabilities. Presence of MXene serves to hinder the initiation of unwanted side reactions of cathode material. Additionally, the adaptable layered structure of MXene contributes to enhancing the mechanical characteristics (control volume expansion during cycling process) of the NCM811 cathode. Energy Dispersive X-ray Spectroscopy (EDS) mapping further indicate the presence and distribution of Ni, Mn, Co, Ti, C and O elements. Presence of Ti and C elements show MXene successfully coated on cathode material.

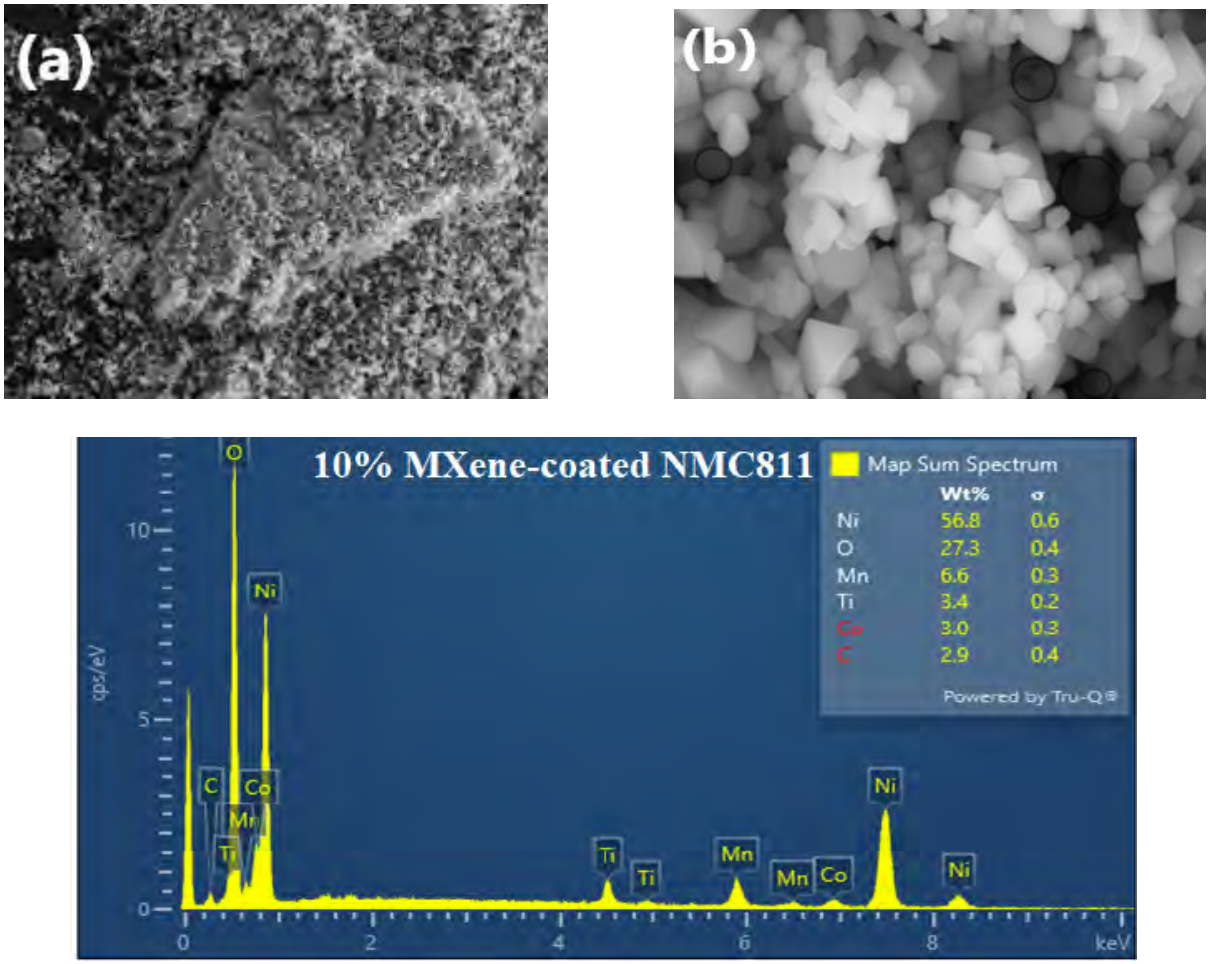

Figure 4.8 SEM and EDS spectrum of NMC811-$Ti_3C_2T_x$ (coated NMC811) 10% of NMC811

4.3 Cyclic Voltammetry

A cyclic voltammetry (CV) analysis was conducted on (NMC811) cathode material, MXene ($Ti_3C_2T_x$) and NMC811-($Ti_3C_2T_x$) nanocomposite using a Gamry machine. The CV-tests were performed in a three-electrode system, where the electrodes were connected to a computer. Nickel foam was employed as the active electrode. This electrode was immersed in a 1 M solution of lithium chloride (LiCl) electrolyte. The research involved conducting (cyclic voltammetry) analysis. Cyclic Voltammetry (CV) experiments were performed using a Gamry machine to analyze the behavior of pristine (NMC811) cathode material, $Ti_3C_2T_x$ (MXene) and MXene coated NMC811 (NMC811-$Ti_3C_2T_x$). The potential window ranged from -0.6V to 0.6V, and the scan rates varied from 10mV/s to 100mV/s. The results indicated distinct oxidation (anodic peaks) and reduction (cathodic peaks) responses, which are summarized in Table 4.1 for NMC811 and Table 4.2 for MXene, respectively. First cycle of de-lithiation (Li^+ extract from anode and move towards cathode, called discharging) occur at 0.338V and lithiation (Li^+ extract from cathode and move towards anode, called charging) occur at -.052V

and -0.16V with different discharging and charging current values. The oxidation peaks observed during the cycles correspond to the transformation of the material from the high-capacity hexagonal (H-M) phase to the lower-capacity monoclinic (M-H) phase and further to Hexagonal-1to Hexagonal-2 phases. These phase transformations occurring during the charging and discharging processes are identified as the main reason for the unstable cycle life performance. Moreover, at a scan rate of 10mV/s, a minimal difference of 0.16V is observed between the oxidation (anodic) and reduction (cathodic) peaks. This observation indicates that Li+ ions are being reversibly intercalated and de-intercalated in the $LiNi_{0.8}Co_{0.1}Mn_{0.1}O_2$ cathode material, illustrate good stability during the process. The specific capacitance of each cycle, as indicated by the CV-area, demonstrates the electrochemical activity of the material. Furthermore, the cyclic voltammogram area increases with higher scan rates, indicating its potential as a promising electrode material for future battery applications. This suggests that the material exhibits favorable characteristics for energy storage and holds promise for use in advanced battery technologies.

For MXene all cycles of anodic peak observed at 0.44V and cathodic peak observed at ~0.3V with almost constant current values which indicates reversible behaviour of Li^+/Li. MXene coated NMC811 (NMC811-$Ti_3C_2T_x$) exhibit higher specific capacity on 10mV/s rate than individually pristine (NMC811) and MXene ($Ti_3C_2T_x$). Specific capacitance of 10mV/ of CV-area demonstrates best electrochemical activity of (NMC811-$Ti_3C_2T_x$) nanocomposite.

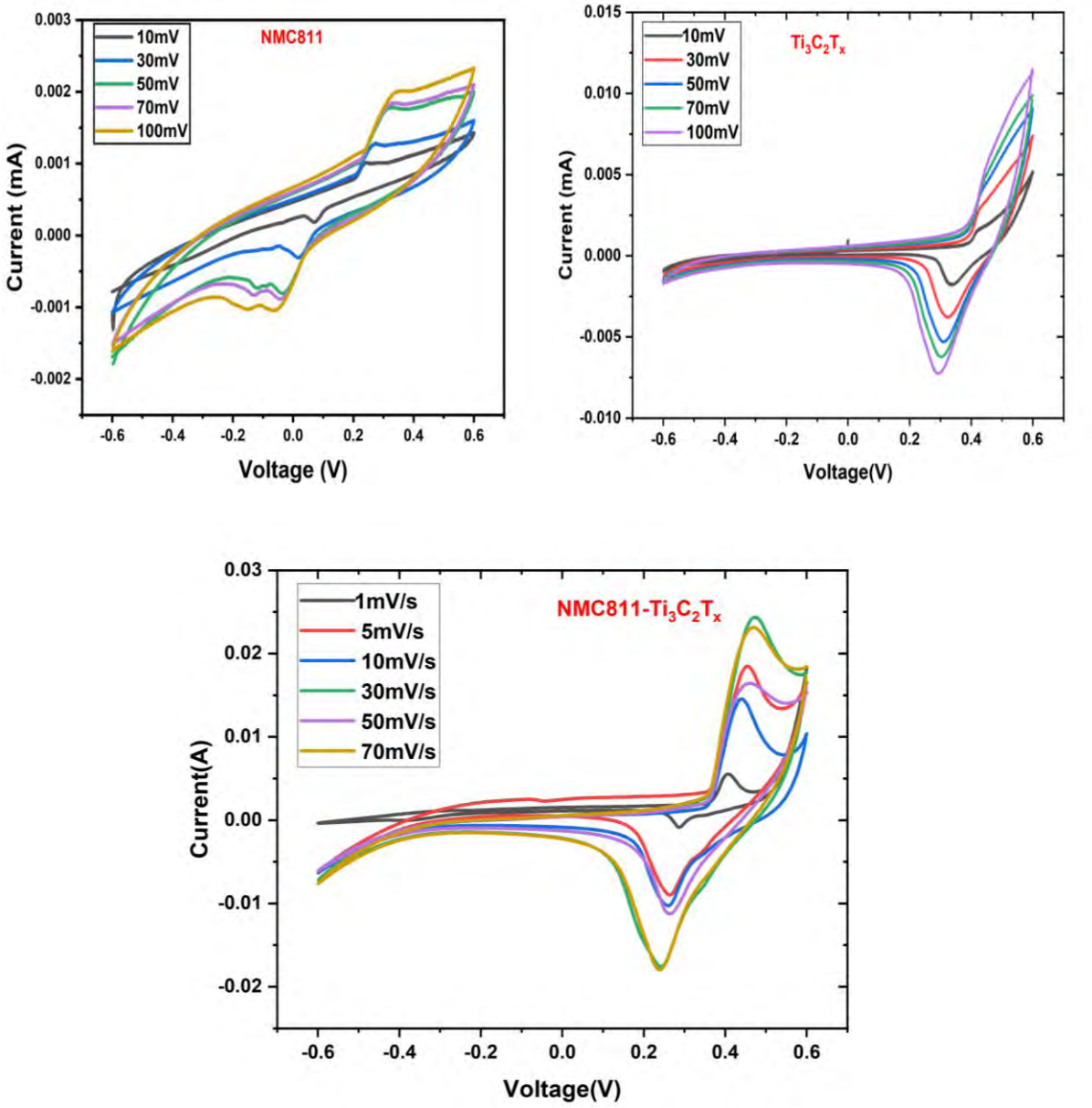

Figure 4.9 Cyclic voltammetry of pristine NMC811, MXene ($Ti_3C_2T_x$) and nano-composite of (NMC811-$Ti_3C_2T_x$) at different scan rate with potential window of -0.6V to 0.6V respectively.

Table 4.1 CV measurements of cathode material (NMC811)

$LiNi_{0.8}Mn_{0,1}Co_{0.1}O_2$ (NMC811)	**Scan-rate mV/s**	**Anodic peaks (V)**	**Cathodic peaks (V)**	**Current-at Anode peaks (A)**	**Current-at cathode peaks (A)**
1st cycle	100	0.338	-0.052, -0.16	0.00197	-0.001
2nd cycle	70	0.312	-0.052, -0.13	0.0018	$-8.5x10^{-4}$
3rd cycle	50	0.314	-0.040, -0.12	0.0018	$-8.0x10^{-4}$
4th cycle	30	0.264	0.014, -0.08	0.0012	$-3.0x10^{-4}$
5th cycle	20	0.256	0.046, -0.060	0.0011	$-5.5x10^{-5}$
6th cycle	10	0.23	0.067, -0.038	0.0010	$-1.87x10^{-4}$

Table 4.2 CV measurements of MXene ($Ti_3C_2T_x$)

MXene ($Ti_3C_2T_x$)	**Scan-rate mV/s**	**Anodic peaks (V)**	**Cathodic peaks (V)**	**Current-at anode peaks (A)**	**Current-at cathode peaks (A)**
1st cycle	100	0.443	0.287	0.005219	-0.007221
2nd cycle	70	0.437	0.296	0.0044	0.0061
3rd cycle	50	0.426	0.303	0.0039	-0.0052
4th cycle	30	0.4117	0.324	0.0028	-0.0038
5th cycle	10	0.415	0.336	0.0014	-0.0018

4.4 EIS Analysis

Electrochemical Impedance Analysis was conducted on (NMC811) cathode material, MXene ($Ti_3C_2T_x$) and NMC811-($Ti_3C_2T_x$) nanocomposite using a Gamry machine. Figure 4.10 clearly show that charge transfer resistance (Rct) of NMC811-$Ti_3C_2T_x$ smaller than that of pristine NMC811 electrode material. Nyquist plots demonstrated that $Ti_3C_2T_x$ coating on electrode materials improve the lithium transportation, which leads to small electrochemical interface impedance and is beneficial to the rate capability.

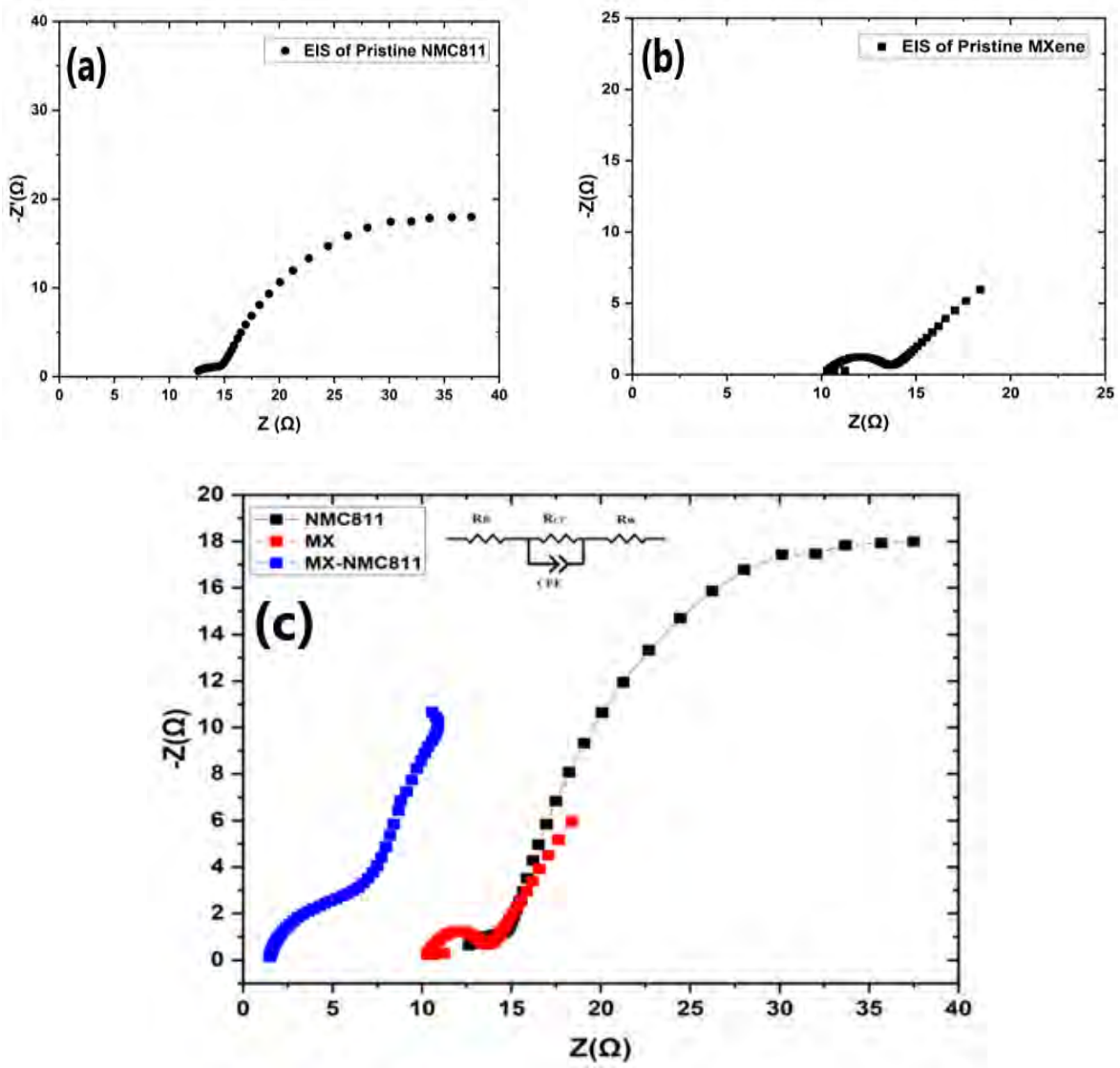

Figure 4.10 The Nyquist plots of pristine NMC811 and $Ti_3C_2T_x$ materials, and stacked plots of both materials with composite (10% $Ti_3C_2T_x$ coated NMC811)

Chapter No. 5

Conclusion

Lithium-ion battery nickel rich cathode material $LiNi_{0.8}Mn_{0.1}Co_{0.1}O_2$ (NMC811) successfully synthesized by co-precipitation and solid-state reaction method. For improving electrochemical performance and solving problems of cathode, MXene coating employ on it that was prepared by molten salt etching method. (NMC811) cathode material characterized by XRD, SEM and CV techniques. XRD demonstrate cathode material crystallinity with hexagonal layered rhombohedral R-3m space group. Average crystallite size of the pure (NMC811) and ($Ti_3C_2T_x$ -NMC811) is 50nm and 33nm respectively was measured. Peaks intensity ratio more than 1.2 indicate lower cation (Ni^{4+}, Ni^{2+}/Li^{+}) mixing in electrolyte. Morphology and particles size investigated by (SEM) technique demonstrate that nanoparticles made in cubic, spherical, and hexagonally shape, while elemental composition of Ni, Mn, Co and O with desired transition molar ratio 8:1:1 in pristine (NMC811) and Ni, Ti, C, Mn, O and Co homogeneously distribution in MXene coated (NMC811) was revealed by EDS spectrum. Conductivity of pure (NMC811) and ($Ti_3C_2T_x$-NMC811) electrodes checked by cyclic voltammetry (CV) under potential window of (-0.6 to 0.6) at different scan rate between 1mV/s to 100mV/s to study redox behaviour. MXene coated (NMC811) cathode exhibit higher specific capacity than pristine (NMC811) cathode. We observed oxidation and reduction on electrodes by study pattern of CV-curve confirmed our material is applicable for rechargeable battery applications, while EIS Nyquist plot of cathode composite with MXene shows minimum resistance between electrode/electrolyte interface surface in a electrolyte during charging and discharging.

References

[1] S. F. Tie and C. W. Tan, “A review of energy sources and energy management system in electric vehicles,” *Renew. Sustain. Energy Rev.*, vol. 20, pp. 82–102, 2013, doi: 10.1016/j.rser.2012.11.077.

[2] X. Wang, X. Lu, B. Liu, D. Chen, Y. Tong, and G. Shen, “Flexible energy-storage devices: Design consideration and recent progress,” *Adv. Mater.*, vol. 26, no. 28, pp. 4763–4782, 2014, doi: 10.1002/adma.201400910.

[3] A. Manthiram, “An Outlook on Lithium Ion Battery Technology,” *ACS Cent. Sci.*, vol. 3, no. 10, pp. 1063–1069, 2017, doi: 10.1021/acscentsci.7b00288.

[4] H. Konishi *et al.*, “Improvement of electrochemical performance of nickel-manganese-based lithium-rich layer-structured cathode material by controlling lithium/transition-metal ratio,” *Solid State Ionics*, vol. 327, pp. 39–46, 2018, doi: 10.1016/j.ssi.2018.10.017.

[5] M. Ghiji *et al.*, “A review of lithium-ion battery fire suppression,” *Energies*, vol. 13, no. 19, 2020, doi: 10.3390/en13195117.

[6] D. Deng, “Li-ion batteries: basics, progress, and challenges,” *Energy Sci. Eng.*, vol. 3, no. 5, pp. 385–418, 2015.

[7] J. W. Fergus, “Recent developments in cathode materials for lithium ion batteries,” *J. Power Sources*, vol. 195, no. 4, pp. 939–954, 2010, doi: 10.1016/j.jpowsour.2009.08.089.

[8] H. J. Noh, S. Youn, C. S. Yoon, and Y. K. Sun, “Comparison of the structural and electrochemical properties of layered Li[NixCoyMnz]O2 (x = 1/3, 0.5, 0.6, 0.7, 0.8 and 0.85) cathode material for lithium-ion batteries,” *J. Power Sources*, vol. 233, pp. 121–130, 2013, doi: 10.1016/j.jpowsour.2013.01.063.

[9] L. Li *et al.*, “Recent progress on electrolyte functional additives for protection of nickel-rich layered oxide cathode materials,” *J. Energy Chem.*, vol. 65, pp. 280–292, 2022, doi: 10.1016/j.jechem.2021.05.049.

[10] S. S. Mukrimaa *et al.*, “No 主観的健康感を中心とした在宅高齢者における 健康関連指標に関する共分散構造分析Title,” *J. Penelit. Pendidik. Guru Sekol. Dasar*,

vol. 6, no. August, p. 128, 2016, doi: GUBGMHVpwcTsPFvNNVdG5DKtpv6UwksAfzw5aULcGzgG.

[11] B. Robert and E. B. Brown, “No 主観的健康感を中心とした在宅高齢者における健康関連指標に関する共分散構造分析Title,” no. 1, pp. 1–14, 2004, doi: https://www.researchgate.net/publication/265064873_Energy_Storage_Technology_Review.

[12] C. A. Russell, “The electrochemical theory of Sir Humphry Davy: Part I: The voltaic pile and electrolysis,” *Ann. Sci.*, vol. 15, no. 1, pp. 1–13, 1959, doi: 10.1080/00033795900200018.

[13] Q. Wang, J. Li, H. Jin, S. Xin, and H. Gao, “Prussian-blue materials: Revealing new opportunities for rechargeable batteries,” *InfoMat*, vol. 4, no. 6, 2022, doi: 10.1002/inf2.12311.

[14] X. Miao, H. Ni, H. Zhang, C. Wang, J. Fang, and G. Yang, “Li2ZrO3-coated 0.4Li2MnO 3·0.6LiNi1/3Co1/3Mn1/3O 2 for high performance cathode material in lithium-ion battery,” *J. Power Sources*, vol. 264, pp. 147–154, 2014, doi: 10.1016/j.jpowsour.2014.04.068.

[15] A. Yoshino, “The birth of the lithium-ion battery,” *Angew. Chemie - Int. Ed.*, vol. 51, no. 24, pp. 5798–5800, 2012, doi: 10.1002/anie.201105006.

[16] H. Schiffer and A. Guerra, “Electricity and Vital Force: Discussing the Nature of Science Through a Historical Narrative,” *Sci. Educ.*, vol. 24, no. 4, pp. 409–434, 2015, doi: 10.1007/s11191-014-9718-6.

[17] J. Wen, Y. Yu, and C. Chen, “A review on lithium-ion batteries safety issues: Existing problems and possible solutions,” *Mater. Express*, vol. 2, no. 3, pp. 197–212, 2012, doi: 10.1166/mex.2012.1075.

[18] V. Ponce, D. E. Galvez-Aranda, and J. M. Seminario, “Analysis of a Li-Ion Nanobattery with Graphite Anode Using Molecular Dynamics Simulations,” *J. Phys. Chem. C*, vol. 121, no. 23, pp. 12959–12971, 2017, doi: 10.1021/acs.jpcc.7b04190.

[19] C. Liang *et al.*, “Obstacles toward unity efficiency of LiNi1-2xCoxMnxO2 (x = 0 ~ 1/3) (NCM) cathode materials: Insights from ab initio calculations,” *J. Power Sources*, vol. 340, pp. 217–228, 2017, doi: 10.1016/j.jpowsour.2016.11.056.

[20] D. Kundu, E. Talaie, V. Duffort, and L. F. Nazar, “The emerging chemistry of sodium ion batteries for electrochemical energy storage,” *Angew. Chemie - Int. Ed.*, vol. 54, no. 11, pp. 3432–3448, 2015, doi: 10.1002/anie.201410376.

[21] A. K. C. Estandarte *et al.*, “Operando Bragg Coherent Diffraction Imaging of LiNi0.8Mn0.1Co0.1O2Primary Particles within Commercially Printed NMC811 Electrode Sheets,” *ACS Nano*, vol. 15, no. 1, pp. 1321–1330, 2021, doi: 10.1021/acsnano.0c08575.

[22] J. Cho, Y. J. Kim, and B. Park, “Novel LiCoO2 cathode material with Al2O3 coating for a Li ion cell,” *Chem. Mater.*, vol. 12, no. 12, pp. 3788–3791, 2000, doi: 10.1021/cm000511k.

[23] Y. Idemoto, T. Mochizuki, K. Ui, and N. Koura, “Properties, Crystal Structure, and Performance of o-LiMnO[sub 2] as Cathode Material for Li Secondary Batteries,” *J. Electrochem. Soc.*, vol. 153, no. 2, p. A418, 2006, doi: 10.1149/1.2142293.

[24] S. Komaba, S. T. Myung, N. Kumagai, T. Kanouchi, K. Oikawa, and T. Kamiyama, “Hydrothermal synthesis of high crystalline orthorhombic LiMnO2 as a cathode material for Li-ion batteries,” *Solid State Ionics*, vol. 152–153, pp. 311–318, 2002, doi: 10.1016/S0167-2738(02)00320-X.

[25] J. C. Garcia *et al.*, “Surface Structure, Morphology, and Stability of Li(Ni1/3Mn1/3Co1/3)O2 Cathode Material,” *J. Phys. Chem. C*, vol. 121, no. 15, pp. 8290–8299, 2017, doi: 10.1021/acs.jpcc.7b00896.

[26] N. V. Kosova, N. F. Uvarov, E. T. Devyatkina, and E. G. Avvakumov, “Mechanochemical synthesis of LiMn2O4 cathode material for lithium batteries,” *Solid State Ionics*, vol. 135, no. 1–4, pp. 107–114, 2000, doi: 10.1016/S0167-2738(00)00288-5.

[27] Y. Li *et al.*, “Leaf-like V2O5 nanosheets fabricated by a facile green approach as high energy cathode material for lithium-ion batteries,” *Adv. Energy Mater.*, vol. 3, no. 9, pp. 1171–1175, 2013, doi: 10.1002/aenm.201300188.

[28] Y. Xie, H. T. Yu, T. F. Yi, and Y. R. Zhu, “Understanding the thermal and mechanical stabilities of olivine-type LiMPO4 (M = Fe, Mn) as cathode materials for rechargeable lithium batteries from first principles,” *ACS Appl. Mater. Interfaces*, vol. 6, no. 6, pp.

4033–4042, 2014, doi: 10.1021/am4054833.

[29] J. Xu, S. Dou, H. Liu, and L. Dai, “Cathode materials for next generation lithium ion batteries,” *Nano Energy*, vol. 2, no. 4, pp. 439–442, 2013, doi: 10.1016/j.nanoen.2013.05.013.

[30] R. N. Ramesha, D. Bosubabu, M. G. Karthick Babu, and K. Ramesha, “Tuning of Ni, Mn, and Co (NMC) content in 0.4(LiNixMnyCozo2)·0.4(Li2MnO3) toward stable high-capacity lithium-rich cathode materials,” *ACS Appl. Energy Mater.*, vol. 3, no. 11, pp. 10872–10881, 2020, doi: 10.1021/acsaem.0c01897.

[31] S. Zhao, K. Yan, J. Zhang, B. Sun, and G. Wang, “Reaction Mechanisms of Layered Lithium-Rich Cathode Materials for High-Energy Lithium-Ion Batteries,” *Angew. Chemie - Int. Ed.*, vol. 60, no. 5, pp. 2208–2220, 2021, doi: 10.1002/anie.202000262.

[32] S. Zhao *et al.*, “Towards high-energy-density lithium-ion batteries: Strategies for developing high-capacity lithium-rich cathode materials,” *Energy Storage Mater.*, vol. 34, pp. 716–734, 2021, doi: 10.1016/j.ensm.2020.11.008.

[33] F. Meng, X. Xiong, L. Tan, B. Yuan, and R. Hu, “Strategies for improving electrochemical reaction kinetics of cathode materials for subzero-temperature Li-ion batteries: A review,” *Energy Storage Mater.*, vol. 44, pp. 390–407, 2022, doi: 10.1016/j.ensm.2021.10.032.

[34] H. Widiyandari, A. N. Sukmawati, H. Sutanto, C. Yudha, and A. Purwanto, “Synthesis of LiNi0.8Mn0.1Co0.1O2 cathode material by hydrothermal method for high energy density lithium ion battery,” *J. Phys. Conf. Ser.*, vol. 1153, no. 1, 2019, doi: 10.1088/1742-6596/1153/1/012074.

[35] Q. Lin *et al.*, “A new insight into continuous performance decay mechanism of Ni-rich layered oxide cathode for high energy lithium ion batteries,” *Nano Energy*, vol. 54, pp. 313–321, 2018, doi: 10.1016/j.nanoen.2018.09.066.

[36] Z. . Liu and Z. Zhu, “In Situ Probing Characterization of Ni-Rich Nmc811 Thin Film Prepared by Sol-Gel Method in Different Scanning Probe Microscopy Techniques,” *SSRN Electron. J.*, 2022, doi: 10.2139/ssrn.4096080.

[37] T. Or, S. W. D. Gourley, K. Kaliyappan, A. Yu, and Z. Chen, “Recycling of mixed cathode lithium-ion batteries for electric vehicles: Current status and future outlook,”

Carbon Energy, vol. 2, no. 1, pp. 6–43, 2020, doi: 10.1002/cey2.29.

[38] K. Märker, P. J. Reeves, C. Xu, K. J. Griffith, and C. P. Grey, "Evolution of Structure and Lithium Dynamics in LiNi0.8Mn0.1Co0.1O2 (NMC811) Cathodes during Electrochemical Cycling," *Chem. Mater.*, vol. 31, no. 7, pp. 2545–2554, 2019, doi: 10.1021/acs.chemmater.9b00140.

[39] J. Z. Kong *et al.*, "Enhanced electrochemical performance of Ni-rich LiNi0.6Co0.2Mn0.2O2 coated by molecular layer deposition derived dual-functional C-Al2O3 composite coating," *J. Alloys Compd.*, vol. 799, pp. 89–98, 2019, doi: 10.1016/j.jallcom.2019.05.330.

[40] A. L. Hoskins *et al.*, "Nonuniform Growth of Sub-2 Nanometer Atomic Layer Deposited Alumina Films on Lithium Nickel Manganese Cobalt Oxide Cathode Battery Materials," *ACS Appl. Nano Mater.*, no. 12, pp. 6989–6997, 2019, doi: 10.1021/acsanm.9b01490.

[41] Y. Di Xu *et al.*, "Improving cycling performance and rate capability of Ni-rich LiNi0.8Co0.1Mn0.1O2 cathode materials by Li4Ti5O12 coating," *Electrochim. Acta*, vol. 268, pp. 358–365, 2018, doi: 10.1016/j.electacta.2018.02.049.

[42] C. Xiong, H. Fu, L. Wu, and G. Yuan, "Enhanced electrochemical performance of LiNi0.8Co0.1Mn0.1O2 Cathode Material for lithium ion batteries by WO3 surface coating," *Int. J. Electrochem. Sci.*, vol. 15, no. 9, pp. 8990–9002, 2020, doi: 10.20964/2020.09.60.

[43] J. Liang *et al.*, "Coating Ni-rich cathode with an amorphous carbon for improving the stability and electrochemical performance," *Compos. Commun.*, vol. 36, 2022, doi: 10.1016/j.coco.2022.101356.

[44] X. Ren *et al.*, "Localized high-concentration sulfone electrolytes for high-efficiency lithium-metal batteries," *Chem*, vol. 4, no. 8, pp. 1877–1892, 2018.

[45] Z. Fohlerova, K. Kamnev, M. Sepúlveda, Z. Pytlicek, J. Prasek, and A. Mozalev, "Nanostructured Zirconium-Oxide Bioceramic Coatings Derived from the Anodized Al/Zr Metal Layers," *Adv. Mater. Interfaces*, vol. 8, no. 14, p. 2100256, 2021.

[46] M. Jeong, H. Kim, W. Lee, S.-J. Ahn, E. Lee, and W.-S. Yoon, "Stabilizing effects of Al-doping on Ni-rich LiNi0. 80Co0. 15Mn0. 05O2 cathode for Li rechargeable

batteries," *J. Power Sources*, vol. 474, p. 228592, 2020.

[47] F. Schipper *et al.*, "From surface ZrO2 coating to bulk Zr doping by high temperature annealing of nickel-rich lithiated oxides and their enhanced electrochemical performance in lithium ion batteries," *Adv. Energy Mater.*, vol. 8, no. 4, p. 1701682, 2018.

[48] C. Wang, X. Ma, J. Cheng, L. Zhou, J. Sun, and Y. Zhou, "Effects of Ca doping on the electrochemical properties of LiNi0. 8Co0. 2O2 cathode material," *Solid State Ionics*, vol. 177, no. 11–12, pp. 1027–1031, 2006.

[49] K. Park, H. Jung, L. Kuo, P. Kaghazchi, C. S. Yoon, and Y. Sun, "Improved cycling stability of Li [Ni0. 90Co0. 05Mn0. 05] O2 through microstructure modification by boron doping for Li-ion batteries," *Adv. energy Mater.*, vol. 8, no. 25, p. 1801202, 2018.

[50] W. Xiang *et al.*, "Synergistic coupling effect of sodium and fluorine co-substitution on enhancing rate capability and cycling performance of Ni-rich cathode for lithium ion battery," *J. Alloys Compd.*, vol. 786, pp. 56–64, 2019.

[51] Y.-D. Xu *et al.*, "Stabilizing the structure of nickel-rich lithiated oxides via Cr doping as cathode with boosted high-voltage/temperature cycling performance for Li-ion battery," *Energy Technol.*, vol. 8, no. 1, p. 1900498, 2020.

[52] F. A. Susai *et al.*, "Improving performance of LiNi0. 8Co0. 1Mn0. 1O2 cathode materials for lithium-ion batteries by doping with molybdenum-ions: theoretical and experimental studies," *ACS Appl. energy Mater.*, vol. 2, no. 6, pp. 4521–4534, 2019.

[53] M. Eilers-Rethwisch, M. Winter, and F. M. Schappacher, "Synthesis, electrochemical investigation and structural analysis of doped Li [Ni0. 6Mn0. 2Co0. 2-xMx] O2 (x= 0, 0.05; M= Al, Fe, Sn) cathode materials," *J. Power Sources*, vol. 387, pp. 101–107, 2018.

[54] T. He *et al.*, "The effects of alkali metal ions with different ionic radii substituting in Li sites on the electrochemical properties of Ni-Rich cathode materials," *J. Power Sources*, vol. 441, p. 227195, 2019.

[55] S. Wang, M. Yan, Y. Li, C. Vinado, and J. Yang, "Separating electronic and ionic conductivity in mix-conducting layered lithium transition-metal oxides," *J. Power*

Sources, vol. 393, pp. 75–82, 2018.

[56] L. Jiang, Q. Wang, and J. Sun, "Electrochemical performance and thermal stability analysis of LiNixCoyMnzO2 cathode based on a composite safety electrolyte," *J. Hazard. Mater.*, vol. 351, pp. 260–269, 2018.

[57] J. Chen *et al.*, "Molten Salt-Shielded Synthesis (MS3) of MXenes in Air," *Energy Environ. Mater.*, vol. 6, no. 2, p. e12328, 2023.

[58] Y. Wei, P. Zhang, R. A. Soomro, Q. Zhu, and B. Xu, "Advances in the synthesis of 2D MXenes," *Adv. Mater.*, vol. 33, no. 39, p. 2103148, 2021.

[59] X. Han *et al.*, "Interfacial nitrogen engineering of robust silicon/MXene anode toward high energy solid-state lithium-ion batteries," *J. Energy Chem.*, vol. 67, pp. 727–735, 2022.

[60] Q.-S. Rao, S.-Y. Liao, X.-W. Huang, Y.-Z. Li, Y.-D. Liu, and Y.-G. Min, "Assembly of MXene/PP separator and its enhancement for Ni-Rich LiNi0. 8Co0. 1Mn0. 1O2 electrochemical performance," *Polymers (Basel).*, vol. 12, no. 10, p. 2192, 2020.

[61] W. Liu *et al.*, "Significantly improving cycling performance of cathodes in lithium ion batteries: the effect of Al2O3 and LiAlO2 coatings on LiNi0. 6Co0. 2Mn0. 2O2," *Nano Energy*, vol. 44, pp. 111–120, 2018.

[62] Z.-K. Fang, Y.-R. Zhu, T.-F. Yi, and Y. Xie, "Li4Ti5O12–LiAlO2 composite as high performance anode material for lithium-ion battery," *ACS Sustain. Chem. Eng.*, vol. 4, no. 4, pp. 1994–2003, 2016.

[63] S.-Y. Liao *et al.*, "A multifunctional MXene additive for enhancing the mechanical and electrochemical performances of the LiNi 0.8 Co 0.1 Mn 0.1 O 2 cathode in lithium-ion batteries," *J. Mater. Chem. A*, vol. 8, no. 8, pp. 4494–4504, 2020.

[64] C. Tian, F. Lin, and M. M. Doeff, "Electrochemical characteristics of layered transition metal oxide cathode materials for lithium ion batteries: surface, bulk behavior, and thermal properties," *Acc. Chem. Res.*, vol. 51, no. 1, pp. 89–96, 2017.

[65] Z. C. Shao, J. Guo, Z. Zhao, J. Xia, M. Ma, and Y. Zhang, "Preparation and properties of Al2O3-doping LiNi1/3Co1/3Mn1/3O2 cathode materials," *Mater. Manuf. Process.*, vol. 31, no. 8, pp. 1004–1008, 2016.

[66] Z.-D. Huang, X.-M. Liu, S.-W. Oh, B. Zhang, P.-C. Ma, and J.-K. Kim, "Microscopically porous, interconnected single crystal LiNi 1/3 Co 1/3 Mn 1/3 O 2 cathode material for Lithium ion batteries," *J. Mater. Chem.*, vol. 21, no. 29, pp. 10777–10784, 2011.

[67] H. Darjazi, S. J. Rezvani, S. Brutti, and F. Nobili, "Improvement of structural and electrochemical properties of NMC layered cathode material by combined doping and coating," *Electrochim. Acta*, vol. 404, p. 139577, 2022.

[68] L. Peng, Y. Zhu, U. Khakoo, D. Chen, and G. Yu, "Self-assembled LiNi1/3Co1/3Mn1/3O2 nanosheet cathodes with tunable rate capability," *Nano Energy*, vol. 17, pp. 36–42, 2015.

[69] P. K. Nayak, J. Grinblat, M. Levi, Y. Wu, B. Powell, and D. Aurbach, "TEM and Raman spectroscopy evidence of layered to spinel phase transformation in layered LiNi1/3Mn1/3Co1/3O2 upon cycling to higher voltages," *J. Electroanal. Chem.*, vol. 733, pp. 6–19, 2014.

[70] J. Xu, S.-L. Chou, Q. Gu, H.-K. Liu, and S.-X. Dou, "The effect of different binders on electrochemical properties of LiNi1/3Mn1/3Co1/3O2 cathode material in lithium ion batteries," *J. Power Sources*, vol. 225, pp. 172–178, 2013.

[71] Z. Liu, Z. Zhang, Y. Liu, L. Li, and S. Fu, "Facile and scalable fabrication of K+-doped Li1. 2Ni0. 2Co0. 08Mn0. 52O2 cathode with ultra high capacity and enhanced cycling stability for lithium ion batteries," *Solid State Ionics*, vol. 332, pp. 47–54, 2019.

[72] Xin, F., Zhou, H., Chen, X., Zuba, M., Chernova, N., Zhou, G., & Whittingham, M. S. (2019). Li–Nb–O coating/substitution enhances the electrochemical performance of the LiNi0. 8Mn0. 1Co0. 1O2 (NMC 811) cathode. *ACS applied materials & interfaces*, *11*(38), 34889-34894.

[73] Thapaliya, B. P., Misra, S., Yang, S. Z., Jafta, C. J., Meyer III, H. M., Bagri, P., ... & Dai, S. (2022). Enhancing cycling stability and capacity retention of NMC811 cathodes by reengineering interfaces via electrochemical fluorination. *Advanced Materials Interfaces*, *9*(18), 2200035.